非依存的な筋機能低下者が少なからず存在する．また50歳代以降では，単位筋重量あたりの握力の値は男性と比較して女性で低値となり[8]，女性で筋力の低下は深刻となる．

3) 液性因子

成長ホルモン（GH）の作用により肝臓でインスリン様成長因子（IGF）-1の分泌が起こる．GH/IGF-1がもつ筋タンパク質合成作用は，高齢期における筋萎縮抑制に寄与すると考えられている．しかしながら，視床下部や脳下垂体の機能は加齢とともに低下し，GH/IGF-1は減少する[9]．またGHの分泌を促進する因子として，胃から主に分泌されるグレリンがある[10]．グレリンは摂食亢進作用や抗炎症作用をもつなど，サルコペニアと関連すると考えられている．グレリンは加齢や[11]胃の全摘出などにより減少する[12]．

男性ホルモンであるテストステロンの加齢性の減少は，サルコペニアの発症と強く関連する．NILS-LSAに参加した中高齢男性を対象に，血中の遊離テストステロン濃度と筋量サルコペニアとの関連について検討を行ったところ，遊離テストステロン濃度正常群（7.7pg/mL以上）に対する低下群（7.7pg/mL未満）の筋量サルコペニアのオッズ比は約1.83（95%信頼区間：1.04-3.22）であった[13]．女性を対象とした場合でも，血中の遊離テストステロン濃度が低値であるほど，筋量サルコペニアのオッズ比は上昇する結果となっている[14]．

腫瘍壊死因子α（TNF-α）やインターロイキン（IL）などの炎症性サイトカインは加齢により増加し，筋量の減少や筋機能の低下を誘導すると考えられている[15]．NILS-LSAの調査では，女性において，血中CRP濃度の軽度上昇と下肢筋パワーとの間に関連があることを報告している[16]．

4) 遺伝子

遺伝子単一の影響を評価することは難しく，他の遺伝子の影響や，性差，生活習慣要因など，さまざまな要因を調整した検討が必要となる．

NILS-LSAでは，中高齢男性を対象に遊離テストステロンとアンドロゲン受容体遺伝子（AR）-CAGリピートとの交互作用がSMIに与える影響を検討している[17]．その結果，AR-CAGリピートが23回未満の群では，SMIは遊離テストステロン濃度と関連を示さないのに対し，CAGリピートが23回以上の群では，SMIは遊離テストステロン濃度と関連を認めた（図3）．

日本人中高年女性を対象に，α-アクチニン3：R577X遺伝子多型と大腿部の筋断面積との関連を身体活動量や栄養摂取状況などを調整して検討した研究では，大腿部の筋断面積はXX型がRRおよびRX型と比較して高値を示したことが報告されている[18]．

23歳～85歳までの日本人成人男女を対象に，トランスフォーミング増殖因子-β1：T29C遺伝子多型と除脂肪量の関連を検討した研究では，男性においてCT/TT

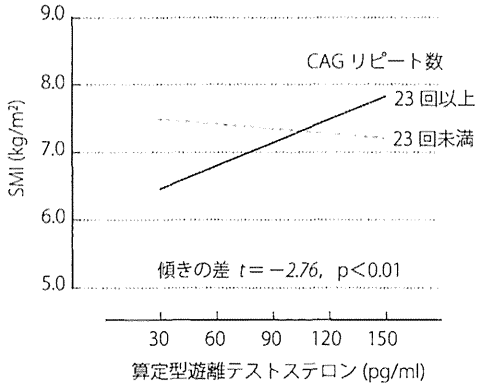

図 3　筋量と遊離テストステロンとの関連にアンドロゲン受容体遺伝子多型が及ぼす影響

中高齢男性 461 名を対象に，従属変数に SMI，独立変数に算定型遊離テストステロン，遺伝子型および両者の交互作用を投入し，年齢，喫煙習慣，総摂取エネルギー量，余暇身体活動量，糖尿病既往歴で調整した一般線型モデルで解析した[18]．アンドロゲン受容体における CAG リピート数が多い場合，筋量はテストステロン依存的に変動するのに対し，CAG リピート数が少ない場合では，筋量は遊離テストステロン濃度の影響を受けない．

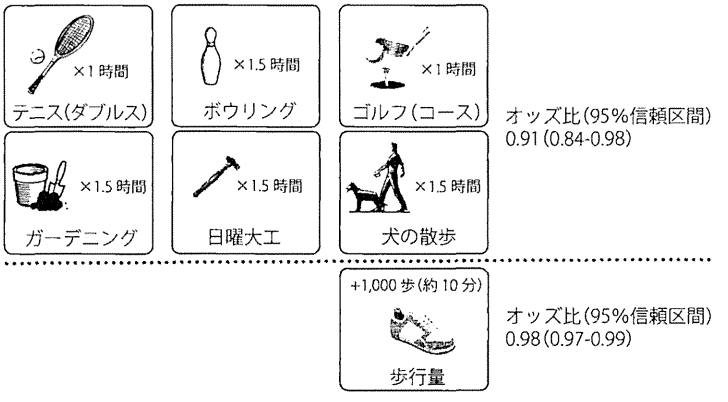

図 4　筋量サルコペニアと関連する 1 日あたりの身体活動量

文献 20, 29 をもとに作成.
オッズ比は筋量サルコペニアを示す．いずれも量反応関係にあり，身体活動量を積み増すことによりサルコペニアのリスクのさらなる低減をはかることができる．

型では CC 型と比較して四肢の除脂肪量は低値を示すことを報告している[19]．一方，女性では閉経状態にある女性でのみ，上肢の除脂肪量と関連が認められている[19]．

5) 身体活動

加齢に伴い日常の活動量は低下する傾向にある．運動不足や長期臥床などの不活動が，筋萎縮や筋力低下を誘導することは経験的に知られてきた．一方で，サルコペニアが引き起こす運動機能の低下が身体活動量を低下させることもあり，両者の因果関係は有症者の生活習慣などをふまえて考える必要がある．いずれにせよ，不活動はさらなる身体機能の低下を引き起こし，身体機能の低下はさらなる不活動を招くといった悪循環に陥ることになる．

NILS-LSA の調査では，一日の身体活動量または歩行量は筋量サルコペニアと関連することが明らかとなっている（**図 4**）[20]．また，NILS-LSA とは異なる日本人高齢者集団を対象とした研究では，25 歳～50 歳までの間に定期的な運動習慣があったと回答した群の筋量サルコペニアのオッズ比は，運動習慣がなかったと回答した群に対して 0.53（95%信頼区間：0.31-0.90）となり[21]，定期的な運動習慣の保有が筋

量サルコペニアの予防に効果的である可能性が示唆されている．

一般的な概念として，レジスタンストレーニングなどの高強度負荷運動が筋力の保持に必要と考えられてきた．一方で，近年ではウォーキングを用いた軽強度負荷運動が，高齢者の筋力の低下の予防や改善に有効であることが示唆されており[22]，今後の研究の進展が期待される．

6) 疾患

心不全や慢性閉塞性肺疾患，がんなどはカヘキシア（悪液質）を誘導し，筋量減少を主とする高度の体重減少を引き起こすことが知られている[23]．

インスリン抵抗性の高い群では低い群と比較して筋量は少ないことが報告されている[24]．そして，糖尿病が引き起こす網膜症などの合併症は高齢者の身体活動を制限する要因となり，サルコペニアを増悪する可能性がある．

7) 栄養

NILS-LSA の調査では，総タンパク質や分岐鎖アミノ酸の摂取量が多いほど筋量サルコペニアのリスクは有意に低下することが明らかとなっている[20]．しかしながら通常は，加齢に伴いタンパク質摂取量は減少する[25]．また，国民健康栄養調査におけるタンパク質の摂取量の年次推移をみると，60 歳以上では 1995 年以降減少が続いており[25]，タンパク質の摂取量が不足している高齢者数は増加している可能性が高い．

n-3 系脂肪酸の一種であるエイコサペンタエン酸は，TNF-αから筋細胞を保護する効果があり[26]，海外では n-3 系脂肪酸の追加摂取により筋タンパク質合成能は上昇することが報告されている[27]．しかしながら，日本人高齢者では魚肉の摂取量が多く，サルコペニアの誘因とはなりにくい可能性もある．

日本人高齢者を対象とした場合，ビタミン D 摂取量は筋量サルコペニアと関連は認められていない[20]．一方，ビタミン D の摂取量や血中濃度は，筋力や身体機能と関連を認めるなど[20, 28]，その影響は筋量と筋機能で異なる可能性がある．

このほかに，腸管機能低下による吸収不良や食欲の減退，また咀嚼，嚥下機能の低下などにも注意をはらう必要がある．

4 おわりに

加齢や性，遺伝子の影響は本人の努力ではどうすることもできない．したがって，運動，栄養改善，疾患など，生活習慣に起因する問題について改善を図ることが，サルコペニアのリスクを低減させるうえで肝要と思われる．

参考文献

1) Fried LP, Tangen CM, et al : Cardiovascular Health Study Collaborative Research Group. Frailty in older adults : evidence for a phenotype. *J Gerontol A Biol Sci Med Sci*, 56 (3) : M146-56, 2001.
2) Baumgartner RN, Koehler KM, et al : Epidemiology of sarcopenia among the elderly in New Mexico. *Am J Epidemiol*, 147 (8) : 755-763, 1998.
3) Sanada K, Miyachi M, et al : A cross-sectional study of sarcopenia in Japanese men and women : reference values and association with cardiovascular risk factors. *Eur J Appl Physiol*, 110 (1) : 57-65, 2010.
4) 清野 諭, 金 美芝・他：地域在住高齢者の握力による移動能力制限の識別. 体力科学, 60 (3) : 259-268, 2011.
5) 下方浩史, 安藤富士子：日常生活機能と骨格筋量, 筋力との関連 日老医誌, 49 (2) : 195-198, 2012.
6) Shimada H, Suzuki T, et al : Performance-based assessments and demand for personal care in older Japanese people : a cross-sectional study. *BMJ Open*, 3 (4) : e002424, 2013.
7) Cruz-Jentoft AJ, Baeyens JP, et al : European Working Group on Sarcopenia in Older People. Sarcopenia : European consensus on definition and diagnosis : Report of the European Working Group on Sarcopenia in Older People. *Age Ageing*, 39 (4) : 412-423, 2010.
8) Shimokata H, Ando F, et al : Age-related changes in skeletal muscle mass among community-dwelling Japanese-a 12-year longitudinal study. *Geriatr Gerontol Int*. (in press)
9) Giovannini S, Marzetti E, et al : Modulation of GH/IGF-1 axis : potential strategies to counteract sarcopenia in older adults. *Mech Ageing Dev*, 129 (10) : 593-601, 2008.
10) Kojima M, Hosoda H, et al : Ghrelin is a growth-hormone-releasing acylated peptide from stomach. *Nature*, 402 (6762) : 656-660, 1999.
11) Rigamonti AE, Pincelli AI, et al : Plasma ghrelin concentrations in elderly subjects : comparison with anorexic and obese patients. *J Endocrinol*, 175 (1) : R1-5, 2002.
12) Takachi K, Doki Y, et al : Postoperative ghrelin levels and delayed recovery from body weight loss after distal or total gastrectomy. *J Surg Res*, 130 (1) : 1-7, 2006.
13) Yuki A, Otsuka R, et al : Relationship between low free testosterone levels and loss of muscle mass. *Sci Rep*, 3 : 1818, 2013.
14) Yuki A, Otsuka R, et al : Low Free Testosterone Levels are Associated with Loss of Appendicular Muscle Mass in Japanese Community-Dwelling Women. Book of Abstract of 18th annual Congress of the ECSS, 657, 2013.
15) Roubenoff R, Harris TB, et al : Monocyte cytokine production in an elderly population : effect of age and inflammation. *J Gerontol A Biol Sci Med Sci*, 53 (1) : M20-26, 1998.
16) 安藤富士子, 北村伊都子・他：潜在性慢性炎症と中高年者のサルコペニアに関する縦断的検討. 日未病システム学誌, 16 (2) : 250-253, 2010.
17) 幸 篤武, 安藤富士子・他：アンドロゲン受容体遺伝子多型とテストステロンの相互作用が中高齢男性の筋量に与える影響. 体力科学, 62 (6) : 529, 2013
18) Zempo H, Tanabe K, et al : Age differences in the relation between ACTN3 R577X polymorphism and thigh-muscle cross-sectional area in women. *Genet Test Mol Biomarkers*, 15 (9) : 639-643, 2011.
19) Fuku N, Mori S, et al : Association of 29C>T polymorphism in the transforming growth factor-β1 gene with lean body mass in community-dwelling Japanese population. *Geriatr Gerontol Int*, 12 (2) : 292-297, 2012.
20) 下方浩史, 安藤富士子：疫学研究からのサルコペニアとそのリスク－特に栄養との関連 日老医誌, 49 (6) : 721-725, 2012.
21) Akune T, Muraki S, et al : Exercise habits during middle age are associated with lower prevalence of sarcopenia : the ROAD study. Osteoporos Int. (in press)
22) Ozaki H, Loenneke JP, et al : Possibility of leg muscle hypertrophy by ambulation in older adults : a brief review. *Clin Interv Aging*, 8 : 369-375, 2013.
23) Evans WJ, Morley JE, et al : Cachexia : a new definition. *Clin Nutr*, 27 (6) : 793-799, 2008.
24) Lee CG, Boyko EJ, et al : Osteoporotic Fractures in Men Study Research Group : Association between insulin resistance and lean mass loss and fat mass gain in older men without diabetes mellitus. *J Am Geriatr Soc*, 59 (7) : 1217-1224, 2011.
25) 厚生労働省：国民健康・栄養調査. http : //www.mhlw.go.jp/bunya/kenkou/kenkou_eiyou_chousa.html
26) Magee P, Pearson S, et al : The omega-3 fatty acid, eicosapentaenoic acid (EPA) : prevents the damaging effects of tumour necrosis factor (TNF)-alpha during murine skeletal muscle cell differentiation. *Lipids Health Dis*, 18 : 7, 24, 2008.
27) Smith GI, Atherton P, et al : Dietary omega-3 fatty acid supplementation increases the rate of muscle protein synthesis in older adults : a randomized controlled trial. *Am J Clin Nutr*, 93 (2) : 402-412, 2011.
28) Suzuki T, Kwon J, et al : Low serum 25-hydroxyvitamin D levels associated with falls among Japanese community-dwelling elderly. *J Bone Miner Res*, 23 (8) : 1309-1317, 2008.
29) Ainsworth BE, Haskell WL, et al : Compendium of physical activities : an update of activity codes and MET intensities. *Med Sci Sports Exerc*, 32 (9 Suppl) : S498-504, 2000.

RESEARCH ARTICLE

Human Mutation

OFFICIAL JOURNAL
HGVS
HUMAN GENOME VARIATION SOCIETY
www.hgvs.org

Genetic and Epigenetic Characteristics of FSHD-Associated 4q and 10q D4Z4 that are Distinct from Non-4q/10q D4Z4 Homologs

Weihua Zeng,[1,2†] Yen-Yun Chen,[1†] Daniel A. Newkirk,[1] Beibei Wu,[3] Judit Balog,[4] Xiangduo Kong,[1] Alexander R. Ball Jr.,[1] Simona Zanotti,[5] Rabi Tawil,[6] Naohiro Hashimoto,[7] Ali Mortazavi,[2] Silvère M. van der Maarel,[4] and Kyoko Yokomori[1*]

[1]*Department of Biological Chemistry, School of Medicine, University of California, Irvine, California;* [2]*Department of Developmental and Cell Biology, School of Biological Sciences, University of California, Irvine, California;* [3]*Department of Microbiology and Molecular Genetics, School of Medicine, University of California, Irvine, California;* [4]*Center for Human and Clinical Genetics, Leiden University Medical Center, RC Leiden, The Netherlands;* [5]*Neuromuscular Diseases and Neuroimmunology Unit, Muscle Cell Biology Laboratory, Fondazione IRCCS Istituto Neurologico "C. Besta", Milano, Italy;* [6]*University of Rochester Medical Center, Rochester, New York;* [7]*Department of Regenerative Medicine, National Institute for Longevity Sciences, National Center for Geriatrics and Gerontology, Obu, Japan*

Communicated by Jacques S. Beckmann

Received 8 May 2013; accepted revised manuscript 6 May 2014.
Published online 17 May 2014 in Wiley Online Library (www.wiley.com/humanmutation). DOI: 10.1002/humu.22593

ABSTRACT: Facioscapulohumeral dystrophy (FSHD) is one of the most prevalent muscular dystrophies. The majority of FSHD cases are linked to a decreased copy number of D4Z4 macrosatellite repeats on chromosome 4q (FSHD1). Less than 5% of FSHD cases have no repeat contraction (FSHD2), most of which are associated with mutations of *SMCHD1*. FSHD is associated with the transcriptional derepression of *DUX4* encoded within the D4Z4 repeat, and SMCHD1 contributes to its regulation. We previously found that the loss of heterochromatin mark (i.e., histone H3 lysine 9 tri-methylation (H3K9me3)) at D4Z4 is a hallmark of both FSHD1 and FSHD2. However, whether this loss contributes to *DUX4* expression was unknown. Furthermore, additional D4Z4 homologs exist on multiple chromosomes, but they are largely uncharacterized and their relationship to 4q/10q D4Z4 was undetermined. We found that the suppression of H3K9me3 results in displacement of SMCHD1 at D4Z4 and increases *DUX4* expression in myoblasts. The *DUX4* open reading frame (ORF) is disrupted in D4Z4 homologs and their heterochromatin is unchanged in FSHD. The results indicate the significance of D4Z4 heterochromatin in *DUX4* gene regulation and reveal the genetic and epigenetic distinction between 4q/10q D4Z4 and the non-4q/10q homologs, highlighting the special role of the 4q/10q D4Z4 chromatin and the *DUX4* ORF in FSHD.

Hum Mutat 35:998–1010, 2014. © 2014 Wiley Periodicals, Inc.

KEY WORDS: FSHD1; FSHD2; DUX4; H3K9me3; SMCHD1; D4Z4; heterochromatin

Introduction

Facioscapulohumeral dystrophy (FSHD) is an autosomal dominant muscular dystrophy characterized by progressive wasting of facial, shoulder, and upper arm musculature [van der Maarel and Frants, 2005]. The majority of FSHD cases (>95%) are caused by monoallelic partial deletion of D4Z4 repeat sequences at the subtelomeric region of chromosome (chr) 4q (4qter D4Z4) (FSHD1; MIM# 158900) [van der Maarel and Frants, 2005; van der Maarel et al., 2011]. D4Z4 is a 3.3 kb macrosatellite repeat that contains an open reading frame (ORF) for the double-homeobox transcription factor *DUX4* retrogene (MIM# 606009) [Gabriëls et al., 1999; Snider et al., 2010; Geng et al., 2012]. There are only 1–10 D4Z4 repeats in the contracted allele in FSHD1, in contrast to 11–150 copies in the intact allele. In the more rare form of FSHD (<5% of cases), there is no D4Z4 repeat contraction (FSHD2) [van Overveld et al., 2003; de Greef et al., 2010]. A recent study found that the *SMCHD1* gene (MIM# 614982) is mutated in >80% of FSHD2 cases (MIM# 158901) [Lemmers et al., 2012].

FSHD occurs only in individuals with a 4qA haplotype with specific single-nucleotide polymorphisms in the chromosomal region distal to the last D4Z4 repeat (creating a noncanonical polyadenylation signal for the *DUX4* transcript) [Lemmers et al., 2002, 2004, 2007, 2010a] with some exceptions [Scionti et al., 2012]. While multiple transcripts encoding different parts of the DUX4 protein have been identified [Snider et al., 2009], expression of the full-length *DUX4* transcript (*DUX4fl*) is most closely associated with FSHD [Lemmers et al., 2010a; Snider et al., 2010]. Overexpression of *DUX4fl* caused differentiation defects in human myoblasts and mouse C2C12 muscle cells, and FSHD-like phenotypes in zebrafish [Bosnakovski et al., 2008; Vanderplanck et al., 2011; Mitsuhashi et al., 2013]. Furthermore, though the *DUX4fl* expression can occasionally be observed in unaffected individuals at very low levels (suggesting the presence of additional disease modifier genes), activation of a subset of the DUX4fl target genes has been observed

Additional Supporting Information may be found in the online version of this article.

†These authors contributed equally to this work.

*Correspondence to: Kyoko Yokomori, Department of Biological Chemistry, School of Medicine, University of California, Irvine, CA 92697-1700. E-mail: kyokomor@uci.edu

Contract grant sponsors: National Institutes of Health (NS069539 and AR058548); Muscular Dystrophy Association (MDA4026); FSH Society (FSHS-DHY-001, FSHS-DHY-002 and FSHS-22011-05); National Library of Medicine (NIH T15LM07443); Eunice Kennedy Shriver National Institute of Child Health and Human Development (T32-HD060555); National Cancer Institute (NIH T32 CA009054).

in patient cells in multiple studies, supporting the significance of DUX4fl in FSHD [Geng et al., 2012; Jones et al., 2012; Rahimov et al., 2012; Broucqsault et al., 2013; Ferreboeuf et al., 2014].

The chromatin environment plays a significant role in gene regulation in normal development and disease [Feinberg, 2007]. Epigenetic alteration of D4Z4 chromatin was found to be a common link between FSHD1 and FSHD2 [van Overveld et al., 2003; Zeng et al., 2009]. D4Z4 repeats contain transcriptionally repressive heterochromatin harboring DNA hypermethylation and histone H3 lysine 9 trimethylation (H3K9me3) together with H3K27me3 [van Overveld et al., 2003; Zeng et al., 2009]. Using chromatin immunoprecipitation (ChIP) analysis, we found a specific loss of H3K9me3 at the D4Z4 repeat sequences in both FSHD1 and FSHD2 patient proliferating cell cultures [Zeng et al., 2009]. Importantly, this change is highly specific for FSHD; no significant change of H3K9me3 was observed in other muscular dystrophies, some of which share similar clinical phenotypes [Zeng et al., 2009]. This change is seen not only in affected muscle cells, but also in patient fibroblasts from skin biopsies and lymphoblasts from blood samples [Zeng et al., 2009]. This indicates that the loss of H3K9me3 is not an epiphenomenon of dystrophic muscle. Although D4Z4 DNA was also shown to be hypomethylated in FSHD, we showed that the H3K9me3 loss is not a downstream consequence of DNA hypomethylation since H3K9me3 is intact in the phenotypically unrelated immunodeficiency-centromeric instability-facial anomalies syndrome, in which D4Z4 is severely DNA hypomethylated [Zeng et al., 2009] due to mutations in the DNA methyltransferase 3B (*DNMT3B*) gene [Hansen et al., 1999; Xu et al., 1999]. Nevertheless, the loss of DNA methylation and H3K9me3 indicates the perturbation of heterochromatin structure at D4Z4 in FSHD, strongly suggesting that FSHD is an epigenetic abnormality disease associated with the impairment of heterochromatin at D4Z4. We also found that the heterochromatin-binding protein HP1γ and the higher order chromatin organizer cohesin are corecruited to D4Z4 in an H3K9me3-dependent and cell type specific manner, and are lost in FSHD as a consequence of the loss of H3K9me3 [Zeng et al., 2009]. FSHD-specific loss of heterochromatin in this region is thought to contribute to the derepression of *DUX4* [Lemmers et al., 2010a; Snider et al., 2010; Geng et al., 2012]. However, this hypothesis has not been explicitly tested.

Our previous study indicated that loss of H3K9me3 occurs not only at 4q D4Z4, but also at 10q D4Z4 in FSHD1 and FSHD2 [Zeng et al., 2009]. DNA hypomethylation was observed at both 4q and 10q D4Z4 in FSHD2, though it appears to be restricted to the contracted 4q allele in FSHD1 [van Overveld et al., 2003; de Greef et al., 2007, 2009]. The extent of heterochromatin change in other regions of the FSHD genome has not been determined. There are additional D4Z4-like sequences present in several other chromosomes [Hewitt et al., 1994; Winokur et al., 1994; Lyle et al., 1995; Tam et al., 2004]. These D4Z4 homologs are largely uncharacterized, and it is unknown whether they also encode functional *DUX4* genes and undergo similar chromatin changes as do 4q and 10q D4Z4. Understanding the extent of genetic and epigenetic similarity or difference of these homologs is essential to elucidate the disease mechanism, particularly in FSHD2, in which heterochromatin status may be globally altered, and also to properly distinguish the 4q/10q D4Z4-specific events. In this study, we report the effect of the inhibition of H3K9me3 on *DUX4fl* expression and characterization of the non-4q/10q D4Z4 homologs from seven chromosomes. We found that decreased H3K9me3 results in the reduced SMCHD1 binding to D4Z4 and derepression of *DUX4fl* expression, demonstrating the significance of the loss of the H3K9me3 heterochromatin at D4Z4 in gene regulation. While the *DUX4* ORF is highly conserved in 4q/10q D4Z4 repeats, it is frequently disrupted by high degrees of nucleotide polymorphism in the D4Z4 homologs. Furthermore, while H3K9me3/HP1γ/cohesin heterochromatin marks and DNA methylation are also present at these D4Z4 homologs in normal cells, they remain unchanged in both FSHD1 and FSHD2 patient cells. The results reveal that the preservation of the *DUX4* ORF and the unique FSHD-associated epigenetic alterations that contributes to *DUX4* expression are restricted to 4q and 10q D4Z4, indicating their distinct role in FSHD pathogenesis.

Materials and Methods

Cells and DNA Mapping Panel

The NIGMS human/rodent somatic cell hybrid mapping panel #2, version 3 was from Coriell Cell Repositories (Camden, NJ), in which human chrs 1, 16, 17, 20, and 21 hybrids are from mice, whereas the others are from Chinese hamsters. Mouse somatic cell hybrids containing human chrs 4, 10, 13, 14, 15, or 21 (catalog number GM11687, 11688, 11689, 10479, 11715, or 08854, respectively, from Coriell Cell Repositories) were grown in DMEM medium supplemented with 10% FBS, penicillin/streptomycin, and 2 mM L-glutamine. Normal, FSHD1 and FSHD2 myoblasts were grown in F-10 medium (Invitrogen, Carlsbad, CA) supplemented with 20% FBS, 10 ng/ml bFGF (Invitrogen), and 20 ng/ml dexamethasone sodium phosphate (Sigma–Aldrich, St. Louis, MO) except FSHD1 myoblasts (GM17731 and GM17940 from Coriell Cell Repositories) were grown in F-10 medium supplemented with 15% FBS. KD3 human myoblasts immortalized by the expression of telomerase, cyclin D1, and mutated cyclin-dependent kinase 4 are grown as previously described [Shiomi et al., 2011]. Control (NFGr) and FSHD2 (KII-II) fibroblasts were grown in DMEM/F-12 (1:1) supplemented with 10% FBS, 2 mM GlutaMAX-I (Invitrogen-Gibco, Carlsbad, CA), 10 mM HEPES buffer (Invitrogen-Gibco), and 1 mM sodium pyruvate (Invitrogen-Gibco). Control and patient cells used for ChIP analysis are shown in Supp. Table S1.

Antibodies

Antigen affinity-purified rabbit polyclonal antibodies specific for Rad21 and the preimmune IgG control were published previously [Gregson et al., 2001]. Antibodies against HP1γ, H3K9me3, and H3K27me3 were purchased from EMD/Millipore (Billerica, MA). Antibody against 5-methylcytidine (metC) was from Eurogentec North America Inc. (San Diego, CA). SMCHD1 antibody was from Abcam (Cambridge, MA) (ab31865).

Chaetocin, Auranofin, and H_2O_2 Treatment

KD3 myoblasts that reached approximately 80% confluency were treated with 0.4 mM chaetocin (Sigma-Aldrich C9492) and harvested after 24 h. Cells were also treated with the thioredoxin reductase (TrxR) inhibitor auranofin (Sigma-Aldrich A6733) (1 μM) for 24 h or 0.5 mM H_2O_2 for 3 h. The effects of different treatments on D4Z4 H3K9me3 and *DUX4fl* expression were analyzed by ChIP-PCR and RT-nested set PCR as described below.

Lentiviral shRNA Transduction

Nontarget shRNA control (Sigma-Aldrich: SHC002) and the lentiviral shRNA against human SUV39H1 (TRCN0000157251, Sigma-Aldrich) were transfected into 293T cells along with lentiviral

packaging plasmids, using Lipofectamine 2000 (Invitrogen). Supernatants were collected 36 and 60 h posttransfection, passed through a 0.45 μm nitrocellulose filter, and applied on KD3 cells in the presence of polybrene (1 μg/mL). The next day, cells were selected with puromycin for 48 h (2 μg/ml, Sigma). Forty-eight hours after infection, cells were transferred to 10 or 15 cm dishes and maintained 2 days before harvesting for experimental purposes.

DUX4 Nested RT-PCR

Total RNA was extracted using the Qiagen RNeasy Plus kit. Two to five micrograms of RNA was used for double-stranded cDNA synthesis according to manufacturer's protocol (Life Technologies, Grand Island, NY) with the exception of using enzymes purchased from New England Biolabs, Inc. (Ipswich, MA). cDNA was purified by Qiagen PCR purification kit and eluted in 40 μl EB buffer. The nested PCR was done using the primer sets (182–183 and 1A–184) previously published [Snider et al., 2010]. The PCR cycling protocol is as follows: 95°C 2 min, 95°C 30 sec, 62°C 30 sec, 72°C 1 min 40 sec (repeat 34 times), then 72°C 10 min. PCR enhancer system (Invitrogen 11495-017) was used for the nested PCR. The PCR products were loaded on agarose gel and the observed bands were cut out for sequencing to confirm the DUX4 identity. At least three independent experiments were performed and the representative experiment was shown.

ChIP Analysis

The ChIP analysis was performed based on the protocol from the Upstate ChIP assay kit with some modification as previous described [Zeng et al., 2009]. Briefly, we cross-linked the cells with 1% formaldehyde and used 1×10^6 cells for one histone ChIP and 3×10^6 cells for the other ChIP assays. Protein A beads were preincubated with 1 mg/ml BSA and 0.2 mg/ml ssDNA for 20 min at 4°C. Typically, 4 μg IgG was used per assay. The mixtures of antibody and nuclear extracts precleared with protein A beads were incubated at 4°C overnight followed by precipitation with protein A beads. After washing, immunoprecipitated materials were eluted with 0.1 M $NaHCO_3$ and 1% SDS, and cross-links were reversed at 65°C for 4–6 h. The metC ChIP assay was performed according to the previously published protocol [Weber et al., 2005]. Primer sequences are listed in the Supp. Table S2 or were published previously [Zeng et al., 2009]. The endpoint gel analysis of the ChIP-PCR products was carried out using the Luminescent Image Analyzer LAS-4000 (FujiFilm Medical Systems U.S.A., Stamford, CT). Real-time Q-PCR was performed using the iCycler iQ real-time PCR detection system (Bio-Rad Laboratories, Inc., Hercules, CA) with iQ SYBR Green Supermix (Bio-Rad). The ChIP-PCR signal was normalized by the subtraction of the preimmune IgG ChIP-PCR signal, which was further divided by input genomic PCR (for normalization of different D4Z4 or D4Z4 homolog repeat numbers in different cells) minus PCR with no template as previously described [Zeng et al., 2009]. Alternatively, ChIP was normalized with pan-histone H3 antibody ChIP (Abcam ab1791) (Fig. 1D and Supp. Fig. S4) as recently described [Thijssen et al., 2013]. Both normalization methods yielded comparable results.

Genomic- and ChIP-PCR Cloning and Sequencing

The Q-PCR forward (Q-PCR-F) primer and the 4q-Hox reverse (4q-Hox-R) primer [Zeng et al., 2009] were used to amplify a subdomain of the D4Z4 homologs from the mapping panel and somatic cell hybrid genomic DNA with an annealing temperature of 58°C. The PCR enzyme was cloned using Pfu DNA polymerase (Stratagene, La Jolla, CA) and the blunt-end PCR product was ligated into the pCRBlunt vector (Invitrogen). The bacterial colonies transformed with the clones were picked, grown in 96-well plates, and subjected to single-pass plasmid sequencing (Agencourt, Beverly, MA). The total number of clones sequenced for each chromosome was 20 for chr 3, 50 for chr 4, 40 for chr 10, 37 for chr 13, 41 for chr 14, 28 for chr 15, 22 for chr 21, 16 for chr 22, and 18 for chr Y, respectively. Cloning and sequencing analyses of 4q/10q and non-4q/10q D4Z4 repeats were performed using either genomic or H3K9me3 ChIP DNA from multiple human cells. We sequenced 32 clones from four independent cell samples (individuals) for Q-PCR-F + 4q-Hox-R, 41 clones from five individual cell samples for Q-PCR-F + Q-PCR-reverse, 44 clones from five individual cell samples for Q-PCR-F + chr 3-reverse, 50 clones from five individual cell samples for chr 15-forward + 4q-Hox-R, and 136 clones for Q-PCR-F + chr 22-reverse (87 were from genomic DNA and 49 from H3K9me3 ChIP DNA) from 14 different individual cell samples (Supp. Table S3).

Results

Inhibition of H3K9me3 Results in *DUX4fl* Expression and the Loss of SMCHD1 Binding

We previously determined that SUV39H1 histone methyltransferase (HMTase) is responsible for H3K9me3 at D4Z4 in HeLa cells [Zeng et al., 2009]. Based on these results, we treated immortalized human KD3 myoblasts with chaetocin, a SUV39 HMTase inhibitor (Fig. 1). We confirmed that H3K9me3 is present at D4Z4 in this cell line, and found that the chaetocin treatment indeed decreased H3K9me3 at D4Z4 (Fig. 1A, left). Consistent with this, chaetocin treatment resulted in transcriptional derepression of *DUX4fl* (Fig. 1A, right). The identity of the *DUX4fl*-specific PCR product was confirmed by sequencing. Chaetocin was also shown to inhibit TrxR [Tibodeau et al., 2009]. Upregulation of *HMOX1* is a marker for TrxR inhibition [Mostert et al., 2003; Trigona et al., 2006]. We found that *HMOX1* is indeed upregulated in cells treated with chaetocin similar to cells treated with auranofin, a TrxR inhibitor, indicating that chaetocin under our condition also inhibits TrxR (Supp. Fig. S1A). Unlike chaetocin, however, treating cells with auranofin failed to affect H3K9me3 at D4Z4 or *DUX4fl* expression, indicating that the observed chaetocin effect on H3K9me3 and *DUX4fl* expression at D4Z4 is not due to TrxR inhibition (Fig. 1B). Since TrxR inhibition leads to oxidative damage induction [Tibodeau et al., 2009], and oxidative stress has been shown to be associated with FSHD [Turki et al., 2012], we also treated cells with H_2O_2. This failed to exhibit any effect on *DUX4fl* expression, indicating that the chaetocin treatment's effect on *DUX4* expression is not the result of oxidative stress (Fig. 1B, right). Chaetocin was also shown to affect G9a HMTase [Iwasa et al., 2010]. Under our treatment condition, we found that H3K9me3 at the *c-Myc* region, which was shown to be mediated by G9a in HeLa cells [Duan et al., 2005], was also suppressed, suggesting that G9a is also inhibited (Supp. Fig. S1B). Thus, although G9a depletion had no effect on H3K9me3 at D4Z4 in HeLa cells [Zeng et al., 2009], we cannot exclude the possibility that G9a may contribute to D4Z4 heterochromatin organization in the context of myoblasts. Nevertheless, we observed H3K9me3 reduction at D4Z4 in SUV39H1 shRNA-transduced cells, strongly supporting the significant role of SUV39H1 in H3K9me3 at D4Z4 in myoblasts (Fig. 1C). Importantly, SUV39H1 depletion led to *DUX4fl* induction (Fig. 1C, right). Taken together, the results

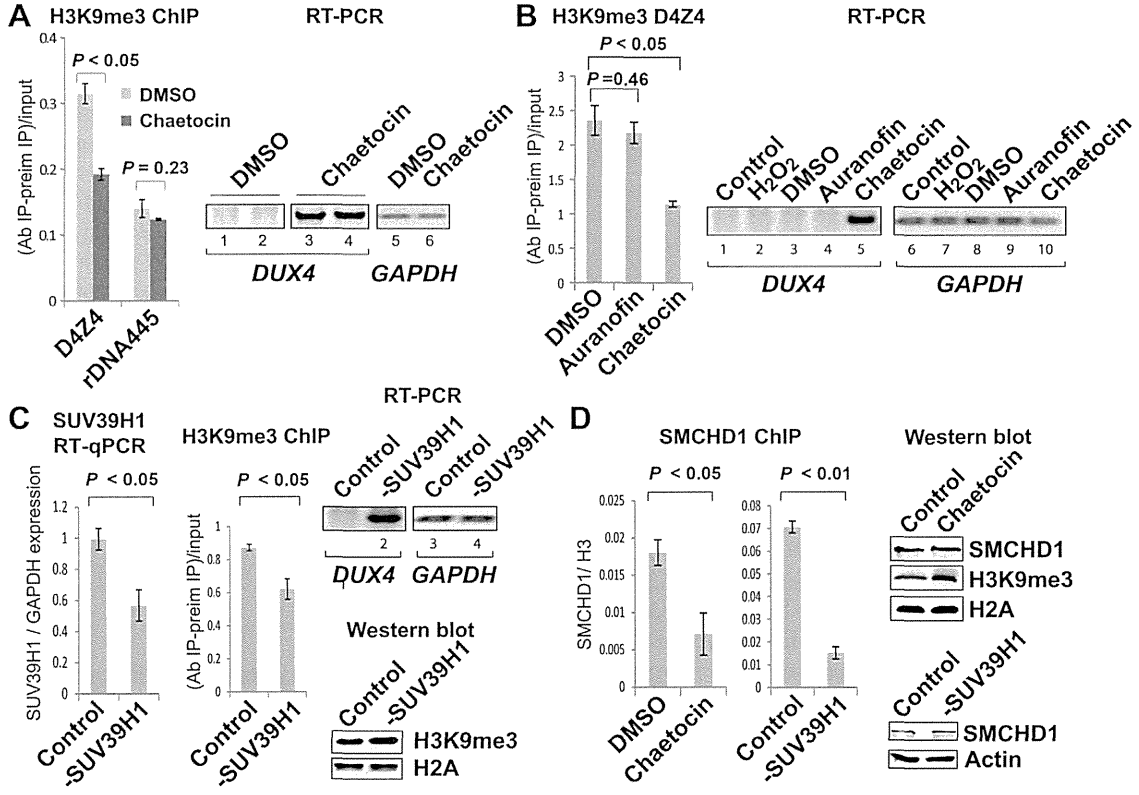

Figure 1. Inhibition of H3K9me3 results in DUX4fl upregulation. **A**: The effect of chaetocin on H3K9me3 at D4Z4 and *DUX4* expression in KD3 human myoblasts. Left: H3K9me3 ChIP-PCR analysis of D4Z4 and rDNA regions in DMSO and chaetocin-treated cells. Right: RT-PCR analysis of *DUX4fl* expression. Nested set RT-PCR analysis of *DUX4fl* expression as described [Snider et al., 2010] in cells treated with DMSO only or chaetocin as indicated at the top. The PCR products were sequenced to confirm their identity. *GAPDH* RT-PCR serves as a control. **B**: Comparison of the effects of chaetocin and auranofin treatments on D4Z4 H3K9me3 and *DUX4* expression. Left: H3K9me3 ChIP-PCR analysis of the D4Z4 region in auranofin- and chaetocin-treated cells. Right: *DUX4fl* and *GAPDH* RT-PCR analyses as in (**A**). Untreated control, H_2O_2, DMSO-treated, auranofin, or cheatocin-treated cells were compared. **C**: The effect of SUV39H1 depletion on D4Z4 H3K9me3 and *DUX4* expression. Lentiviral shRNA against SUV39H1 was used for depletion. Left: RT-qPCR analysis of SUV39H1 depletion in control and SUV39H1 shRNA-treated cells. Middle: ChIP-PCR analysis of H3K9me3 at D4Z4 in control and SUV39H1 shRNA-treated cells. Right: Top, *DUX4fl* and *GAPDH* RT-PCR as in (**A**); Bottom, Western blot analysis of control and SUV39H1-depleted cells with antibodies specific for H3K9me3 and H2A. **D**: ChIP-PCR analysis of SMCHD1 binding at D4Z4 in chaetocin and SUV39H1 shRNA-treated cells. *Y*-axis: (SMCHD1 ChIP–preimmune IgG)/input, which was further normalized by histone H3 ChIP. Right: Western blot analysis of cheatocin (top) or SUV39H1 shRNA (bottom) treated cells compared to DMSO (control) or control shRNA-treated cells, respectively, using antibodies indicated. Histone H2A (top) and actin (bottom) served as a loading control.

indicate that the inhibition of H3K9me3 at D4Z4 under these experimental conditions contributes to the derepression of *DUX4*.

SMCHD1 was found to bind to D4Z4 and depletion of SMCHD1 results in transcriptional derepression of *DUX4fl* [Lemmers et al., 2012]. Since SMCHD1 associates with the H3K9me3 domains of the inactive X chromosomes to modulate chromatin compaction [Nozawa et al., 2013], we tested whether H3K9me3 also dictates SMCHD1 association at D4Z4. Both chaetocin treatment and SUV39H1 shRNA depletion resulted in the significant loss of SMCHD1 binding to D4Z4 (Fig. 1D). Neither treatment affected the SMCHD1 protein level (Fig. 1D, right). Thus, the results indicate that one important downstream effector of H3K9me3 is SMCHD1 and suggest that the loss of H3K9me3 at D4Z4 in FSHD contributes to decreased SMCHD1 binding to D4Z4 leading to *DUX4fl* expression.

Sequencing of Subregions of D4Z4 Homologs on Different Chromosomes

The study of D4Z4 chromatin has been difficult due to the sequence similarity found in the D4Z4-like homologs. Having established the significance of H3K9me3 reduction at D4Z4, we decided to characterize non-4q/10q D4Z4 repeats to see if they also undergo similar epigenetic changes and contribute to *DUX4* expression. We examined these repeats on individual chromosomes separately using a DNA mapping panel and somatic cell hybrids carrying a single human chromosome. We previously designed two pairs of PCR primers (4q-Hox and Q-PCR) that selectively amplify 4q and 10q D4Z4 but not other D4Z4 homologs, enabling specific analysis of 4q and 10q D4Z4 in human cells (Fig. 2) [Zeng et al., 2009]. When Q-PCR-F and 4q-Hox-R primers were used against genomic DNA from a DNA mapping panel, PCR products were also obtained from seven other chromosomes (chrs 3, 13, 14, 15, 21, 22, and Y) (Fig. 2). Cloning and sequencing of these PCR products revealed that they all encompass the overlapping region of D4Z4, corresponding to the 5′-untranslated region (5′-UTR) and 5′ one-third of the *DUX4* ORF (Fig. 3A). These chromosomes were previously reported to contain D4Z4 homologs, with the exception of chr 3 [Lyle et al., 1995]. Thus, we have identified a novel D4Z4 homolog on chr 3. Interestingly, a D4Z4 homolog previously shown to be on chr 1 [Lyle et al., 1995] was not amplified by the selected primers, suggesting that the corresponding region is highly divergent in the chr 1 homolog or that the presence of this homolog on chr 1 is variable.

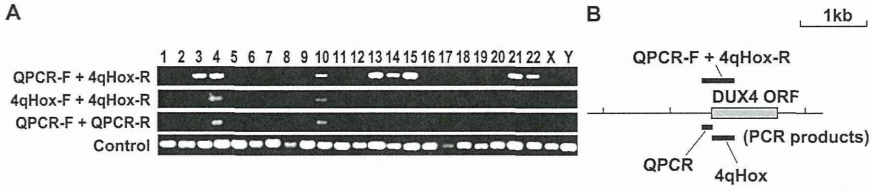

Figure 2. Amplification of the D4Z4 homolog subdomain from chromosomes other than 4q and 10q. **A**: The combination of the Q-PCR forward primer and 4q-Hox reverse primer was used to amplify the D4Z4 homologs on chromosomes 3, 13, 14, 15, 21, 22, and Y from the mapping panel (top panel). The PCR results of the 4q-Hox primer pair and the Q-PCR primer pair, both of which only amplify 4q and 10q D4Z4, are also shown (two middle panels). PCR amplification of mouse β-minor globin or hamster ribosomal DNA repeats serves as an input control (bottom panel). **B**: A schematic diagram of the regions covered by the PCR products as indicated by black bars. The location of the *DUX4* ORF is also shown to demonstrate the relative locations of these PCR products.

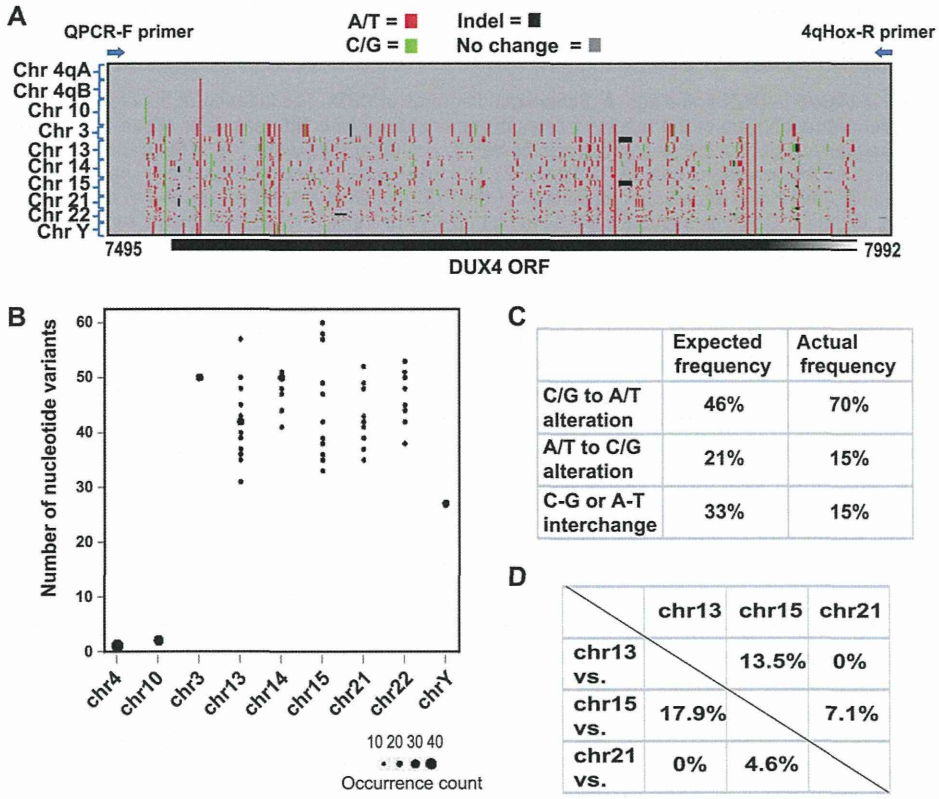

C

	Expected frequency	Actual frequency
C/G to A/T alteration	46%	70%
A/T to C/G alteration	21%	15%
C-G or A-T interchange	33%	15%

D

	chr13	chr15	chr21
chr13 vs.		13.5%	0%
chr15 vs.	17.9%		7.1%
chr21 vs.	0%	4.6%	

Figure 3. The sequence results of the D4Z4 homologs on other chromosomes. **A**: A heat map of the nucleotide variation across sequenced clones. Gray indicates no change, whereas red and green indicate a shift to A/T and C/G, respectively. Black indicates insertion and deletion (indel). The nucleotide numbers are based on the 4q D4Z4 repeat sequence with the accession number AF117653 in the NCBI database. **B**: The occurrence frequency of the D4Z4 homologs with different numbers of nucleotide variants from each individual chromosome. The frequency is indicated by the diameter of the dots used in the plot. **C**: The expected and actual frequency of C/G to A/T alteration, A/T to C/G alteration, and C-G or A-T interchanges on the other D4Z4 homologs in comparison to 4q D4Z4. The expected frequency is calculated based on the nucleotide composition of the sequenced 4q D4Z4 subdomain and the probability of alteration to the other three nucleotides is considered as random. **D**: The percentage of the same sequence present in D4Z4 homologs from different chromosomes. For example, the percentage of "chr 15 versus chr 13" is 17.9%, which means that 17.9% of sequenced clones in chr 15 have sequence(s) that is also present in chr 13.

Non-4q/10q D4Z4 Homologs are Highly Divergent

We sequenced a total of 280 Q-PCR-F + 4q-Hox-R PCR products mentioned above for nine different chromosomes in a DNA mapping panel as well as additional somatic hybrids (see the Methods section for details). We found that the PCR products from 4q and 10q D4Z4 are highly conserved with very little nucleotide variability (Fig. 3A and B, and Supp. Fig. S2). The two major haplotypes of 4q D4Z4 (4qA and 4qB) were shown to differ by one nucleotide (nt) (a "T" instead of "C" at nt 7551 in a portion of 4qB) in this region [Lemmers et al., 2001]. In addition, 10q D4Z4 differs from 4qA D4Z4 by two nucleotides (nts 7515 and 7551, the latter is the same as in 4qB) [Lemmers et al., 2002]. No other heterogeneity was found in 4q and 10q D4Z4-derived clones, consistent with previous reports [Lemmers et al., 2002]. Interestingly, however, cloned PCR products from other homologs exhibited significant nucleotide variability both within and between chromosomes, and none were identical to the 4q or 10q D4Z4 sequences (Fig. 3A and Supp. Fig. S2). Nucleotide changes are scattered relatively evenly throughout

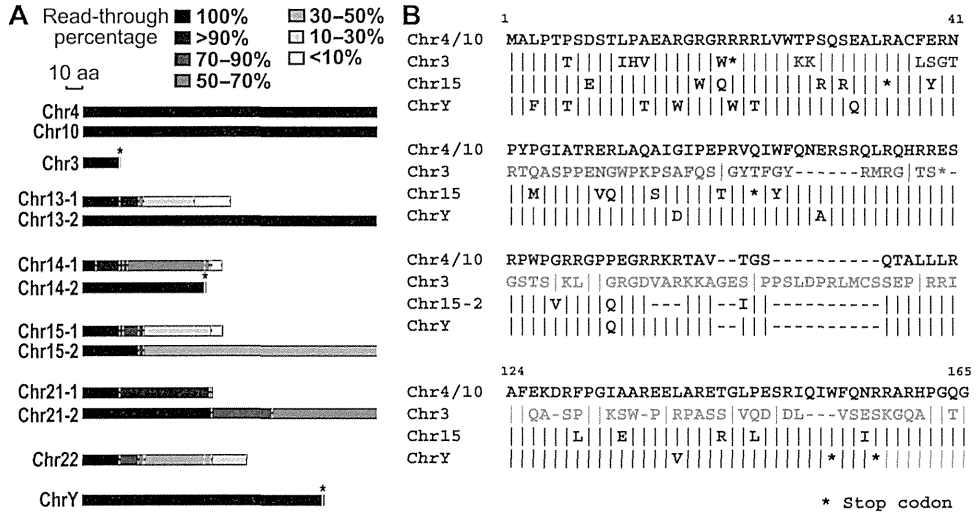

Figure 4. The *DUX4* ORF is closed in D4Z4 homologs. **A**: Schematic diagrams of ORFs. The location of the stop codon is marked by a vertical white dashed line and the read-through ratio of the reading frames is demonstrated with different color codes. For the D4Z4 homologs with the same stop codon in all the sequenced clones, the stop codon is indicated by a vertical solid white line with an asterisk. Two different somatic cell hybrid DNA sources were used for the analysis of chrs 13, 14, 15, and 21, and the results are shown separately. The 4q and 10q *DUX4* ORFs continue beyond the sequenced area. **B**: Amino acid sequence comparison of the PCR-amplified N-terminal regions of 4q/10q DUX4 and corresponding regions derived from chrs 3, 15, and Y. Only one sequence each was found in chrs 3 and Y, while a sequence representing approximately 25% of chr 15–2 from (A) is shown.

the region examined, and there is no apparent mutation hotspot (Fig. 3A). The homologs on chrs 13, 14, 15, 21, and 22 contain multiple sequences with different patterns and degrees of polymorphism, suggesting that the majority of non-4q/10q D4Z4 homologs are susceptible to frequent mutations (Fig. 3B). It should be noted that all PCR clones from chrs 3 and Y each displayed one sequence containing a unique pattern of nucleotide changes (Fig. 3A and B). It is unlikely that this uniformity is due to the existence of only one copy of the D4Z4 homolog on these chromosomes based on the robust PCR signal from chr 3 comparable to that of chr 4 (Fig. 2A). Also, multiple D4Z4 homologs exist on chr Y according to the HG19 build of the human genome reference from the UCSC Genome Browser. Nevertheless, D4Z4 homologs on chrs 3 and Y are divergent from each other and from 4q/10q D4Z4. Furthermore, sequence comparison of the recently discovered single-copy *DUXO* gene on chr 3, which encodes *DUX4c* homolog [Sharon et al., 2012], revealed that the D4Z4 homolog on chr 3 amplified by our primer set is distinct from the *DUXO* gene (Supp. Fig. S3). Taken together, non-4q/10q D4Z4 sequences are highly divergent and variable compared to 4q/10q D4Z4.

D4Z4 Homologs are Enriched for C/G to A/T Conversions and Repeat Exchanges

Approximately 70% of the variation in D4Z4 homologs in comparison to the 4q D4Z4 sequence is a "C" or "G" alteration to "A" or "T" with another 15% corresponding to "A" or "T" alteration to "C" or "G." The remaining 15% variation is C–G (C to G or G to C) or A–T (A to T or T to A) interchanges. These alterations result in about 80% of nucleotide polymorphisms being A or T (Fig. 3A and Supp. Fig. S2). The 4q D4Z4 repeat is a GC-rich sequence (~73% GC), and the sequenced region also contains 68% GC. If the alterations occurred randomly, however, the C/G to A/T alteration ratio should be 46% (Fig. 3C). Thus, there appears to be a bias for A or T conversion in this region in D4Z4 homologs compared to 4q D4Z4.

Despite previous evidence for repeat exchange between 4q and 10q D4Z4 repeats [Cacurri et al., 1998; Zhang et al., 2001; Lemmers et al., 2010a, b], we failed to detect any 4q sequences in 10q clones (n = 48) or 10q patterns in 4q clones (n = 50). Similarly, no 4q or 10q D4Z4 sequences were found in D4Z4 homologs on other chromosomes (n = 182). In contrast, the same nucleotide polymorphism was found in a subset (<20%) of clones from homologs on chrs 13, 15, and 21 (Fig. 3D). In particular, the same pattern of polymorphisms was observed in more than 10% of clones derived from chrs 13 and 15 D4Z4 homologs. Thus, the results suggest that repeat exchanges had occurred at much higher frequency among non-4q/10q D4Z4 homologs than between these homologs and 4q/10q D4Z4.

The *DUX4* ORF is Frequently Disrupted in Non-4q/10q D4Z4 Homologs

The observed hypervariability of the non-4q/10q D4Z4 homologs resulted in alterations of the corresponding amino acid sequence of the putative *DUX4* ORF within the sequenced region. Importantly, in 90% of the D4Z4 homolog clones, the nucleotide polymorphisms introduced nonsense codons (Fig. 4). This is in contrast to clones from 4q and 10q D4Z4, in which the *DUX4* ORF is consistently open. The 4qB haplotype- and 10q-specific nucleotide polymorphisms do not change the *DUX4*-encoded amino acid sequence. Analysis of additional somatic cell hybrids revealed the enrichment of different patterns of mutations, also resulting in *DUX4* ORF interruption, on chrs 14, 15, and 21 (Fig. 4). Taken together, these results reveal that 4q and 10q D4Z4 repeats are unusually conserved compared to non-4q/10q D4Z4 homologs on other chromosomes.

Development and Analysis of D4Z4 Homolog-Specific PCR Primers

Sequence analysis of the D4Z4 homologs from the DNA mapping panel and somatic cell hybrids described above enabled us to design

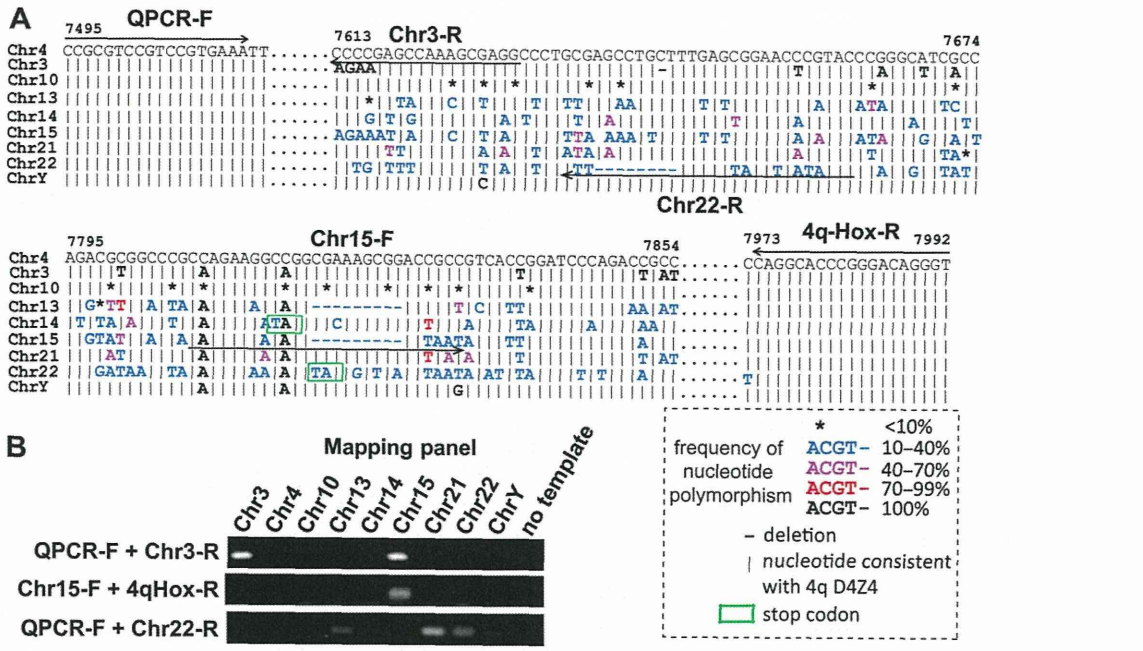

Figure 5. Designing primers specifically covering other D4Z4 homologs. **A**: PCR primers used to amplify D4Z4 homologs on chrs 3, 15, and 22 are indicated by the arrows. **B**: The specificity of the primer pairs was assessed on the mapping panel. Neither 4q nor 10q D4Z4 is amplified with these primer pairs. The positive signals are not restricted to chrs 3 or 22 because some of the non-4q/10q D4Z4 homologs contain the same sequence covered by the primers.

PCR primers specific for their unique regions (Fig. 5A). The specificity of these primer pairs was confirmed using a DNA mapping panel (Fig. 5B). The primer pair Q-PCR-F + chr 3-R amplified D4Z4 homologs from chrs 3 and 15, but not from others (Fig. 5B). Cross-hybridization of the chr 3-R PCR primer with D4Z4 homologs on chr 15 is expected because the same nucleotide variation in the primer-binding region was found in 14.3% of the chr 15-derived clones (Fig. 5A). The primer pair chr 15-F + 4q-Hox-R specifically amplified the D4Z4 homologs from chr 15, although a similar deletion corresponding to the chr 15-F primer-binding site was also found in a subset (8%) of clones from the chr 13-derived D4Z4 homologs (Fig. 5A and B). The primer pair Q-PCR-F + chr 22-R amplified the D4Z4 homologs not only from chr 22, but also from chrs 13 and 21, and more weakly from chrs 14 and Y (Fig. 5B). The chr 22-specific primer corresponds to a unique deletion found in the chr 22 homolog (Fig. 5A). A similar sequence was also found in a subpopulation (15.4%) of clones from chr 21. Although our initial sequencing analyses of the PCR products of the Q-PCR-F + 4q-Hox-R primers did not identify a sequence identical to chr 22 in the chrs 13-, 14-, and Y-derived clones, the presence of the Q-PCR-F +chr 22-R PCR products indicates that a subpopulation of the repeats on these chromosomes contain sufficient homology that allows chr 22-specific primer binding and amplification. The fact that the PCR signals are relatively weak for chrs 14 and Y suggests that they may represent relatively minor copies, which may explain why we did not see this sequence with our limited sequencing. In addition, it is possible that the 4q-HOX-R primer may not be able to bind to some of these repeats with the chr 22-specific primer binding site because of the sequence diversity within the 4q-HOX-R primer binding region. Importantly, there was no amplification of 4q and 10q D4Z4 using these primer pairs, indicating that they selectively amplify non-4q/10q D4Z4 homologs (Fig. 5B and Supp. Table S3).

Epigenetic Analysis of D4Z4 Homologs Using Specific PCR Primers

With 4q/10q and non-4q/10q D4Z4-specific primers, we examined the heterochromatin status of the D4Z4 homologs. A significant decrease of H3K9me3, but not H3K27me3, was observed at 4q/10q D4Z4 in six independent FSHD1 myoblast samples and one FSHD2 myoblast sample compared to four control myoblasts consistent with our previous results [Zeng et al., 2009] (Fig. 6A). A similar decrease of H3K9me3, but not H3K27me3, was observed in FSHD2 fibroblasts [Zeng et al., 2009]. A parallel loss of cohesin and HP1γ binding was also confirmed (Fig. 6B and C). When we used the three sets of homolog-specific PCR primers described above (Fig. 5), the same heterochromatin marks (H3K9me3 and H3K27me3 as well as cohesin and HP1γ binding) were found in control cells, indicating a similar chromatin organization in non-4q/10q D4Z4 homologs as in 4q/10q D4Z4 (Fig. 6). However, no significant decrease in H3K9me3, cohesion, and HP1γ binding was observed at the non-4q/10q homologs in FSHD1 and FSHD2 cells. Although some of the non-4q/10q ChIP signals appeared to be somewhat weaker, the results are variable with some samples even higher than the control. No consistent decrease in H3K9me3 was observed at non-4q/10q homologs in three additional FSHD2 myoblast samples tested (Supp. Fig. S4). D4Z4 DNA is also hypermethylated in normal somatic cells and hypomethylated only at the contracted 4q D4Z4 allele in FSHD1 and at both the 4q and 10q alleles in FSHD2 [van Overveld et al., 2003; de Greef et al., 2007]. Consistent with this, anti-metC ChIP confirmed the decreased DNA methylation at D4Z4 in both FSHD1 and FSHD2 cells, with FSHD2 more severe than FSHD1 (Fig. 6A and C). However, there was no significant decrease in metC in the non-4q/10q D4Z4 homologs. Taken together, the results indicate that heterochromatin marks (including H3K9me3, HP1γ, and cohesin) as well as DNA methylation do not significantly change

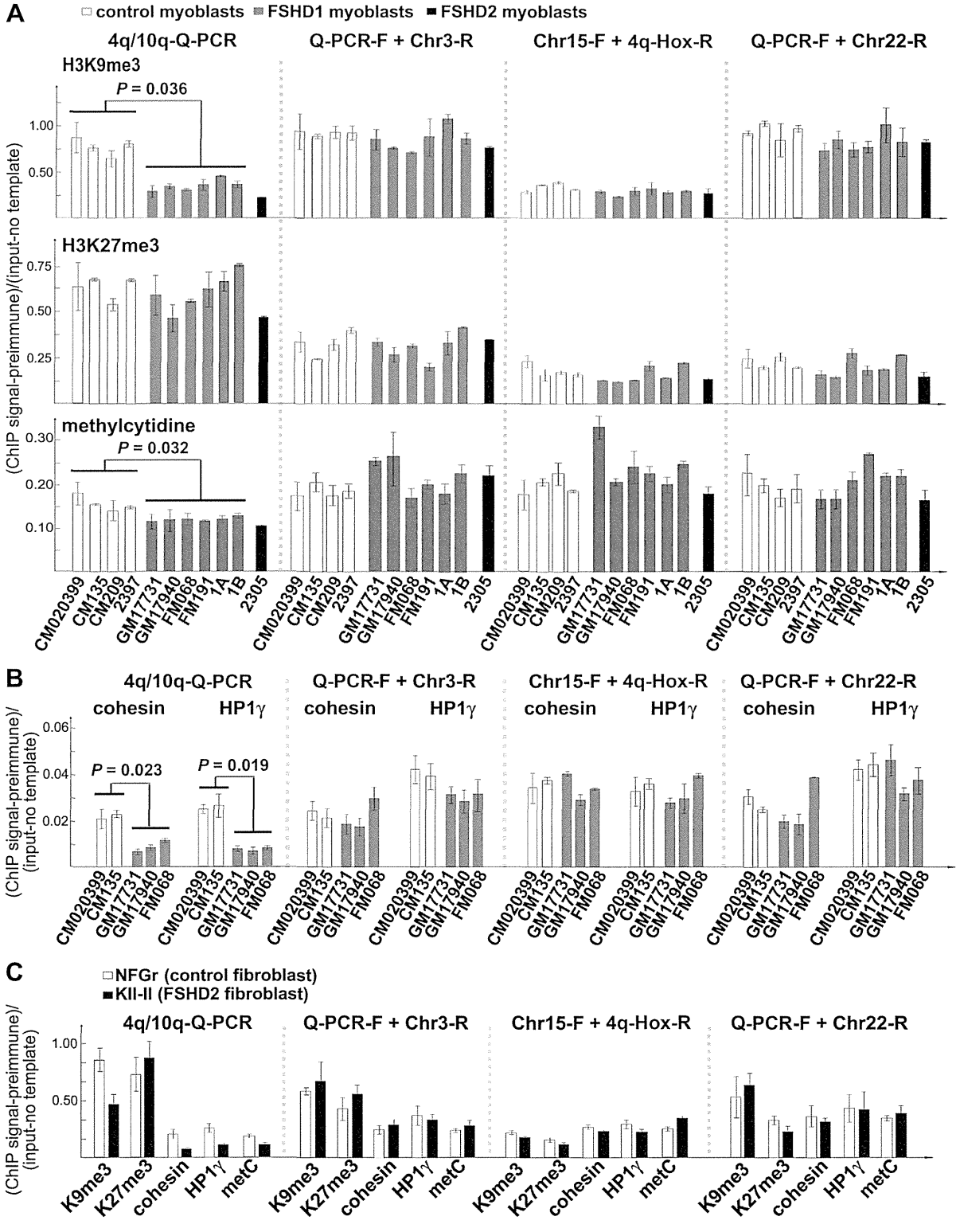

Figure 6. Cohesin/HP1γ binding, H3K9me3, and DNA methylation are intact on non-4q/10q D4Z4 homologs in FSHD1 and FSHD2 cells. **A**: ChIP-qPCR analysis using antibodies specific for H3K9me3, H3K27me3, and methylcytidine (metC) using 4q/10q-specific (4q/10q-Q-PCR) and non-4q/10q-specific (Q-PCR-F + chr 3-R, chr 15-F + 4q-Hox-R, Q-PCR-F + chr 22-R) PCR primers as indicated at the top. Four normal control (white bars), six FSHD1 (grey bars), and one FSHD2 (black bar) myoblast samples were analyzed. The quantitative real-time PCR was normalized with input DNA and preimmune controls as indicated. *P*-values for significant differences between normal and FSHD samples are indicated. **B**: ChIP-qPCR analysis of cohesin and HP1γ in control and FSHD1 myoblasts. **C**: ChIP-qPCR analysis of normal control and FSHD2 fibroblasts using antibodies specific for H3K9me3, H3K27me3, cohesin, HP1γ, and met-C as indicated.

in non-4q/10q D4Z4 homologs in both FSHD1 and FSHD2 cells, demonstrating that the loss of heterochromatin is a restricted event associated only with 4q and 10q D4Z4.

Sequence Analysis of Non-4q/10q D4Z4 Homologs in Multiple Human Cells

Based on the above results, we characterized the sequences of the endogenous non-4q/10q homologs in human cells (Fig. 7). H3K9me3 ChIP or genomic DNA from primary human myoblasts, fibroblasts, and lymphoblasts as well as from the HeLa cervical cancer cell line, all representing different individuals, were used for PCR. The PCR products were cloned and approximately 6–10 clones from each cell sample were sequenced. Interestingly, the 4q and 10q D4Z4 sequences were preferentially amplified from H3K9me3 ChIP DNA using the Q-PCR-F and 4q-Hox-R primers (Fig. 7, top). This primer pair, however, also efficiently amplified non-4q/10q homologs when individual chromosomes were separately available in the DNA mapping panel (Fig. 2). Therefore, the amplification bias may reflect copy number differences in the context of the whole human genome (Fig. 7, top). The Q-PCR-F and Q-PCR-R primers that specifically amplify 4q/10q D4Z4 [Zeng et al., 2009] indeed amplified the identical D4Z4 sequence except for the two SNPs associated with 10q and 4qB. In contrast, similar to the results from the mapping panel and somatic cell hybrids, significant sequence variability was found in the PCR products obtained with the non-4q/10q D4Z4 primers in human cells (Fig. 7 and Supp. Table S3). Approximately 90% of these sequences matched the sequence variations identified in the mapping panel and in the somatic cell hybrids (Figs. 3A and 7, and Supp. Table S3). Chr 15-specific PCR products from five different cell samples (five different individuals) exhibited one identical sequence (Fig. 7, right), in contrast to the highly variable sequences of the Q-PCR-F/chr 22-R PCR products both within and between different cell samples representing 14 different individuals (Fig. 7, bottom). The Q-PCR-F + chr 22-R PCR products from both H3K9me3 ChIP and genomic DNA were highly variable compared to 4q/10q D4Z4 (Fig. 7, bottom). This is consistent with amplification of D4Z4 homologs from multiple chromosomes by this primer pair (Fig. 5B). Over 70% of the sequences of the Q-PCR-F/chr 22-R PCR products lack the start codon for the *DUX4* ORF. Taken together, these results reveal the high conservation of 4q/10q D4Z4 sequences as opposed to non-4q/10q homologs in human cells and confirm that the H3K9me3 heterochromatin mark is indeed present at non-4q/10q homologs. No significant enrichment of a specific sequence(s) in either normal or FSHD cells suggests that H3K9me3 is widely distributed among homologs rather than restricted to a small subregion regardless of the disease status, consistent with the ChIP results (Fig. 6). Our results also demonstrate that these primers are useful for distinguishing 4q/10q from the non-4q/10q D4Z4 repeats in human cells.

Discussion

In the current study, we demonstrated the significance of the H3K9me3 heterochromatin in *DUX4* gene regulation and SMCHD1 assembly at D4Z4. We also performed genomic and epigenomic characterization of the *DUX4* 5′ region in D4Z4 homologs on multiple human chromosomes. Despite awareness of the presence of D4Z4-like repeats scattered on different chromosomes, the extent of their homology and epigenetic similarity with 4q and 10q D4Z4 had not been assessed. We discovered unexpected differences between 4q/10q D4Z4 and other D4Z4 homologs, highlighting the unique link between 4q/10q D4Z4 and FSHD.

H3K9me3 Affects *DUX4fl* Expression and SMCHD1 Binding at D4Z4

Although the loss of H3K9me3 at D4Z4 observed in both FSHD1 and FSHD2 patients was postulated to contribute to disease-specific gene alterations [Zeng et al., 2009], this has not been experimentally proven. We previously demonstrated that SUV39H plays a critical role in mediating H3K9me3 at D4Z4 [Zeng et al., 2009]. Using immortalized myoblasts, we showed that *DUX4fl* expression is indeed increased when H3K9me3 is inhibited either by a chemical inhibitor or by shRNA against SUV39H1. This provides important evidence that H3K9me3 plays a role in *DUX4fl* repression, supporting our hypothesis that disruption of D4Z4 H3K9me3 heterochromatin affects gene expression in FSHD. While these immortalized cells retain differentiation capability in vivo and in vitro with expression of appropriate marker genes [Shiomi et al., 2011], further analysis is necessary to determine to what extent loss of H3K9me3 affects expression of *DUX4* and other genes in the context of primary patient muscle cells and tissues. Furthermore, other H3K9 HMTases, such as G9a, may contribute to H3K9me3 regulation at D4Z4 in a myogenic context, though SUV39H1 depletion alone had a significant effect on *DUX4fl* expression in our study.

SMCHD1, an epigenetic gene silencer mutated in >80% of FSHD2 patients and severe cases of FSHD1, binds to D4Z4 and its depletion results in expression of *DUX4fl* [Lemmers et al., 2012; Sacconi et al., 2013]. How SMCHD1 is recruited to D4Z4 chromatin, however, was unclear. We found that suppression of H3K9me3 affects SMCHD1 association with D4Z4, indicating that SMCHD1 is a component of D4Z4 H3K9me3 heterochromatin. This raises the possibility that SMCHD1 binding to D4Z4 is already impacted by the loss of H3K9me3 in FSHD even in those FSHD1 and FSHD2 cases in which the *SMCHD1* gene is intact, and this may be further worsened in the cases with the haploinsufficiency mutations of SMCHD1. It will be important to test whether SMCHD1 binding to D4Z4 is indeed reduced in primary patient myoblasts. Because SMCHD1 was found to mediate DNA methylation [Ashe et al., 2008; Blewitt et al., 2008; Gendrel et al., 2012], it is possible that SMCHD1 contributes to DNA hypermethylation observed at D4Z4, which is lost in FSHD [van Overveld et al., 2003]. Thus, we propose that H3K9me3 contributes to the recruitment of SMCHD1, which in turn mediates DNA methylation at D4Z4 (Fig. 8A). Although SMCHD1 associates with the inactive X chromosome through interaction with XIST RNA in the chromatin domains enriched for H3K27me3 (though H3K27me3 itself is not required), it also associates with the H3K9me3 domains via the HP1-binding protein HBiX1 [Nozawa et al., 2013]. Thus, it would be interesting to further examine the relationship between SMCHD1 and HP1γ/cohesin that assembles at D4Z4 in an H3K9me3-dependent manner [Zeng et al., 2009]. Taken together, our results suggest that diminished binding of downstream effectors of H3K9me3 may be a key event leading to pathogenic alteration of *DUX4* gene expression (Fig. 8B) and possibly of additional target genes in FSHD.

Frequent Repeat Sharing among D4Z4 Homologs, but Not with 4q/10q D4Z4

Although homologous repeat exchange between 4q and 10q D4Z4 during hominoid evolution has been reported [Lemmers et al., 2010b], we failed to detect any 4q sequence patterns in 10q D4Z4

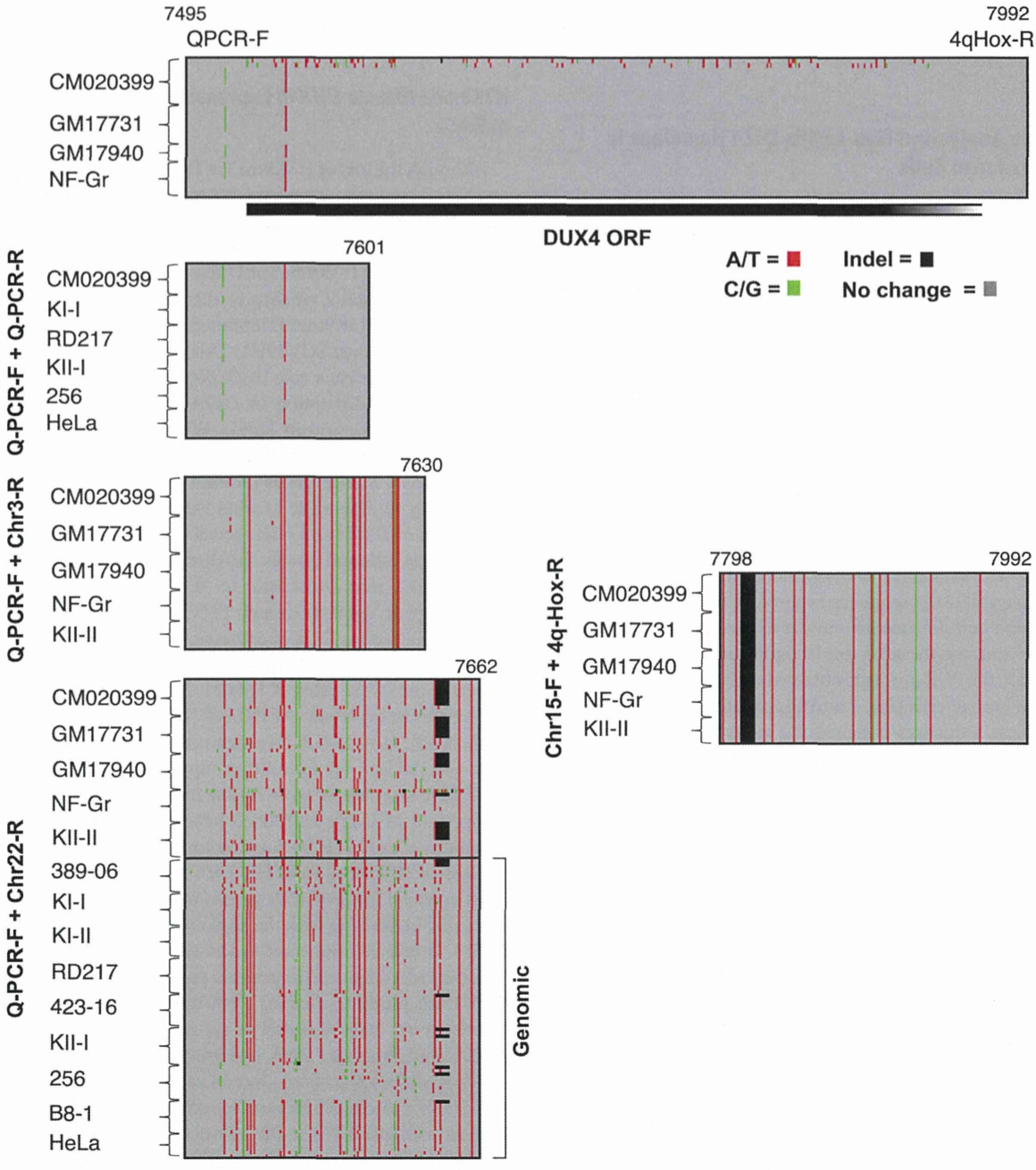

Figure 7. Sequencing analysis of non-4q/10q D4Z4 homologs in human cells. H3K9me3 ChIP and genomic DNA from the indicated human cell samples were used for PCR analysis using 4q/10q-specific (Q-PCR-F + Q-PCR-R) and non-4q/10q homolog-specific (Q-PCR-F + chr 3-R, chr 15-F + 4q-Hox-R, Q-PCR-F + chr 22-R) primers. Sequencing results using Q-PCR and 4q-Hox-R as used in Figure 3A are shown at the top. Nucleotide numbers are indicated. A heat map of the nucleotide variation was made similar to Figure 3A. Gray indicates no change, whereas red and green indicate a shift to A/T and C/G, respectively. Black indicates insertion and deletion (indel). The results are also summarized in the Supp. Table S3. The bracket for each cell line is proportional to the number of clones analyzed.

clones, or vice versa, which may require sequencing of additional DNA samples. In contrast, however, we were able to detect patterns of nucleotide polymorphisms that are shared among non-4q/10q D4Z4 homologs on different chromosomes distinct from 4q/10q D4Z4. This suggests possible evolutionary interactions and repeat exchanges between D4Z4 homologs. We failed to detect any 4q or 10q D4Z4 sequence in the clones from non-4q/10q D4Z4 homologs or vice versa, suggesting that the involvement of 4q/10q D4Z4 repeats in repeat exchange with other D4Z4 homologs is less frequent, consistent with recent observations [Lemmers et al., 2010b]. It should be noted that while 4q and 10q D4Z4 clusters are both in the subtelomeric regions, other D4Z4 homologs are mostly located near centromeres [Lyle et al., 1995]. Furthermore, while 4q/10q D4Z4 repeats are direct repeats, homologs on acrocentric chrs 13, 14, 15, 21, and 22 were shown to be interspersed with ribosomal DNA and β-satellite repeats [Winokur et al., 1996]. Although they are likely to be derived from genomic duplication events, it is possible that differences in chromosomal location and repeat structure

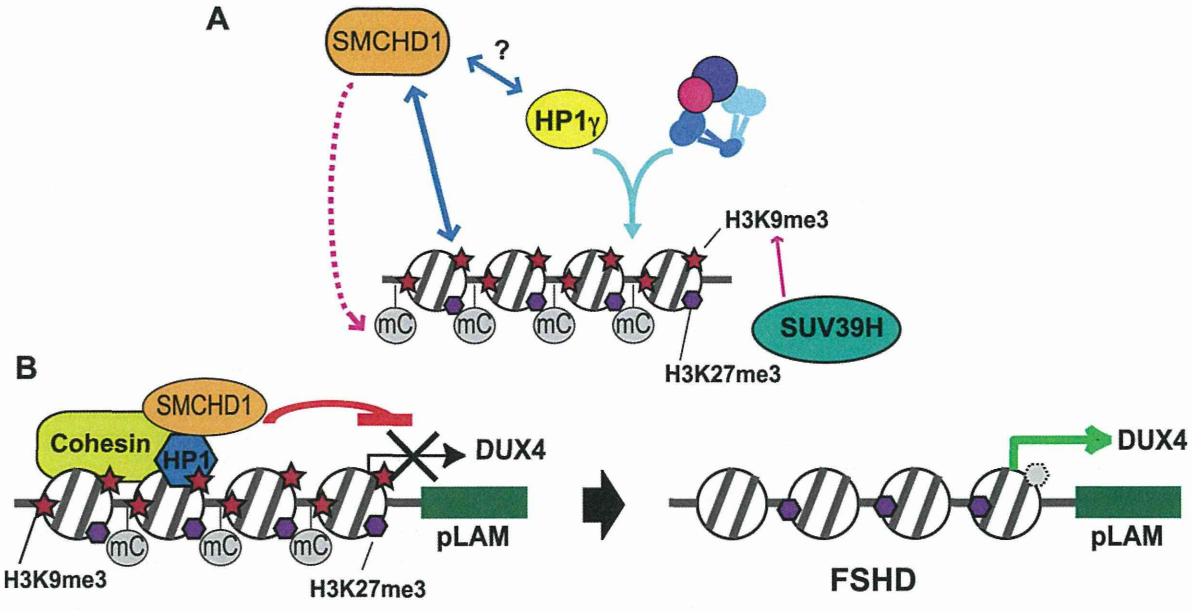

Figure 8. Schematic models of H3K9me3 heterochromatin at D4Z4. **A**: The heterochromatin domain of D4Z4 is marked by DNA hypermethylation, H3K9me3, and K27me3. HP1γ and cohesin are recruited to this region in a mutually dependent manner, which requires H3K9me3 mediated primarily by SUV39H. SMCHD1 is also recruited to this domain in an H3K9me3-dependent manner, and may contribute to DNA methylation. Possible interaction between SMCHD1 and HP1γ is shown with a question mark. **B**: The H3K9me3 heterochromatin assembled at D4Z4 is specifically lost in FSHD, contributing to *DUX4fl* expression.

organization might have restricted the frequency of repeat exchange and interfered with "concerted evolution" [Liao, 1999] between 4q/10q D4Z4 and non-4q/10q homologs.

Hypervariability of D4Z4 Homologs within the *DUX4* Coding Region

Sequence comparison between 4q/10q D4Z4 and other homologs revealed striking differences in the frequency of nucleotide polymorphisms. This was observed not only in the somatic cell hybrids, but also in multiple human cell samples. Many polymorphisms found in non-4q/10q D4Z4 homologs resulted in stop codons in the *DUX4* ORF. The biased C/G to A/T changes in non-4q/10q D4Z4 homologs when compared to 4q/10q D4Z4 sequence may be related to the high frequency of methyl-C to T mutations [Rideout et al., 1990; Mugal and Ellegren, 2011; Xia et al., 2012]. The reason why 4q/10q D4Z4, in particular the *DUX4* ORF, is free from similar mutational changes is currently unclear. Chromosomal location (subtelomeres vs. pericentromeres) or repeat organization (see above) may contribute to this difference. However, it is likely that there is specific selection pressure to preserve the primary sequence and/or the coding capacity of the *DUX4* ORF in 4q and 10q D4Z4. The *DUX4* gene is conserved in primates and is relatively abundantly expressed in human testis [Clapp et al., 2007; Snider et al., 2010], suggestive of its conserved role in development. While D4Z4 transgenic mice failed to exhibit any dystrophic phenotype [Krom et al., 2013], *DUX4fl* and its target gene expression in muscles were nevertheless shown to highly correlate with FSHD in humans [Dixit et al., 2007; Lemmers et al., 2010a; Snider et al., 2010; Geng et al., 2012; Jones et al., 2012; Rahimov et al., 2012; Broucqsault et al., 2013; Ferreboeuf et al., 2014]. Taken together, the results strongly suggest the biological significance of the preservation of the *DUX4* ORF, and support the notion that its misregulation contributes significantly to FSHD.

The Loss of H3K9me3/HP1γ/Cohesin and DNA Methylation at 4q and 10q D4Z4 is Not Transmitted to Other D4Z4 Homologs in FSHD

Using specific PCR primers, we were able for the first time to analyze the epigenetic marks on the non-4q/10q D4Z4 homologs. Although heterochromatin marks similar to those associated with 4q/10q D4Z4 were found on these homologs in control myoblasts/fibroblasts, they are retained in both FSHD1 and FSHD2 cells, suggesting regulatory differences between the heterochromatin of 4q/10q D4Z4 and that of the non-4q/10q D4Z4 homologs in FSHD. In particular, this establishes that even FSHD2, which does not carry any genetic alteration at the 4q D4Z4 locus, exhibits a region-restricted epigenetic change, further emphasizing the specificity and significance of D4Z4 chromatin change in FSHD. Our results indicate that the heterochromatin loss can contribute to derepression of *DUX4* transcription. It is attractive to speculate that this derepression is meaningful, and is therefore associated with the disease, because the *DUX4* ORF on 4q/10q is open. Although we found that the *DUX4* ORF is mostly interrupted in non-4q/10q D4Z4 homologs due to mutations, the 4q D4Z4 region was shown to express the *DUX4* C-terminal short transcript [Snider et al., 2010] and additional noncoding RNA transcripts [Snider et al., 2009], which may still be expressed from the non-4q/10q D4Z4 homologs. The lack of any significant epigenetic change suggests, however, that the expression of these transcripts, if any, from the non-4q/10q D4Z4 homologs is most likely unaffected in FSHD.

Conclusions

Our results indicate that the decrease in H3K9me3, the epigenetic change that signifies FSHD, results in derepression of *DUX4fl* in myoblasts. Our study has revealed a striking difference between 4q/10q D4Z4 and the non-4q/10q D4Z4 homologs on other chromosomes.

The 4q and 10q D4Z4 repeats are highly uniform and conserved, at least in the region encompassing the N-terminus of the *DUX4* ORF, and are epigenetically coregulated in FSHD [Zeng et al., 2009]. In contrast, the corresponding regions in the non-4q/10q homologs are highly heterogeneous with frequent interruptions of the *DUX4* ORF and do not undergo epigenetic alteration in FSHD. Thus, our results reveal the unique characteristics of 4q and 10q D4Z4 among the related repeats, linking the epigenetic alteration and *DUX4* expression in FSHD. The homolog-specific nucleotide polymorphism information reported here should also facilitate further D4Z4 repeat analysis in the FSHD field.

Acknowledgment

We thank Dr. Marina Mora in the Division of Neuromuscular Diseases at the C. Besta Neurological Institute for providing myoblasts through the biobank "Cells, tissues, and DNA from patients with neuromuscular diseases," as part of the Telethon Genetic Network of Biobanks and the EuroBioBank network.

Disclosure statement: The authors declare no conflict of interest.

References

Ashe A, Morgan DK, Whitelaw NC, Bruxner TJ, Vickaryous NK, Cox LL, Butterfield NC, Wicking C, Blewitt ME, Wilkins SJ, Anderson GJ, Cox TC, et al. 2008. A genome-wide screen for modifiers of transgene variegation identifies genes with critical roles in development. Genome Biol 9:R182.

Blewitt ME, Gendrel AV, Pang Z, Sparrow DB, Whitelaw N, Craig JM, Apedaile A, Hilton DJ, Dunwoodie SL, Brockdorff N, Kay GF, Whitelaw E. 2008. SmcHD1, containing a structural-maintenance-of-chromosomes hinge domain, has a critical role in X inactivation. Nat Genet 40:663–669.

Bosnakovski D, Xu Z, Gang EJ, Galindo CL, Liu M, Simsek T, Garner HR, Agha-Mohammadi S, Tassin A, Coppée F, Belayew A, Perlingeiro RR, et al. 2008. An isogenetic myoblast expression screen identifies DUX4-mediated FSHD-associated molecular pathologies. EMBO J 27:2766–2779.

Broucqsault N, Morere J, Gaillard MC, Dumonceaux J, Torrents J, Salort-Campana E, Maues De Paula A, Bartoli M, Fernandez C, Chesnais AL, Ferreboeuf M, Sarda L, et al. 2013. Dysregulation of 4q35- and muscle-specific genes in fetuses with a short D4Z4 array linked to facio-scapulo-humeral dystrophy. Hum Mol Genet 22:4206–4214.

Cacurri S, Piazzo N, Deidda G, Vigneti E, Galluzzi G, Colantoni L, Merico B, Ricci E, Felicetti L. 1998. Sequence homology between 4qter and 10qter loci facilitates the instability of subtelomeric KpnI repeat units implicated in facioscapulohumeral muscular dystrophy. Am J Hum Genet 63:181–190.

Clapp J, Mitchell LM, Bolland DJ, Fantes J, Corcoran AE, Scotting PJ, Armour JA, Hewitt JE. 2007. Evolutionary conservation of a coding function for D4Z4, the tandem DNA repeat mutated in facioscapulohumeral muscular dystrophy. Am J Hum Genet 81:264–279.

de Greef JC, Lemmers RJ, Camaño P, Day JW, Sacconi S, Dunand M, van Engelen BG, Kiuru-Enari S, Padberg GW, Rosa AL, Desnuelle C, Spuler S, et al. 2010. Clinical features of facioscapulohumeral muscular dystrophy 2. Neurology 75:1548–1554.

de Greef JC, Lemmers RJ, van Engelen BG, Sacconi S, Venance SL, Frants RR, Tawil R, van der Maarel SM. 2009. Common epigenetic changes of D4Z4 in contraction-dependent and contraction-independent FSHD. Hum Mol Genet 30:1449–1459.

de Greef JC, Wohlgemuth M, Chan OA, Hansson KB, Smeets D, Frants RR, Weemaes CM, Padberg GW, van der Maarel SM. 2007. Hypomethylation is restricted to the D4Z4 repeat array in phenotypic FSHD. Neurology 69:1018–1026.

Dixit M, Ansseau E, Tassin A, Winokur S, Shi R, Qian H, Sauvage S, Mattéotti C, van Acker AM, Leo O, Figlewicz D, Barro M, et al. 2007. DUX4, a candidate gene of facioscapulohumeral muscular dystrophy, encodes a transcriptional activator of PITX1. Proc Natl Acad Sci USA 104:18157–18162.

Duan Z, Zarebski A, Montoya-Durango D, Grimes HL, Horwitz M. 2005. Gfi1 coordinates epigenetic repression of p21Cip/WAF1 by recruitment of histone lysine methyltransferase G9a and histone deacetylase 1. Mol Cell Biol 25:10338–10351.

Feinberg AP. 2007. Phenotypic plasticity and the epigenetics of human disease. Nature 447:433–440.

Ferreboeuf M, Mariot V, Bessières B, Vasiljevic A, Attié-Bitach T, Collardeau S, Morere J, Roche S, Magdinier F, Robin-Ducellier J, Rameau P, Whalen S, et al. 2014. DUX4 and DUX4 downstream target genes are expressed in fetal FSHD muscles. Hum Mol Genet 23: 171–181.

Gabriëls J, Beckers MC, Ding H, De Vriese A, Plaisance S, van der Maarel SM, Padberg GW, Frants RR, Hewitt JE, Collen D, Belayew A. 1999. Nucleotide sequence of the partially deleted D4Z4 locus in a patient with FSHD identifies a putative gene within each 3.3 kb element. Gene 236:25–32.

Gendrel AV, Apedaile A, Coker H, Termanis A, Zvetkova I, Godwin J, Tang YA, Huntley D, Montana G, Taylor S, Giannoulatou E, Heard E, et al. 2012. Smchd1-dependent and -independent pathways determine developmental dynamics of CpG island methylation on the inactive X chromosome. Dev Cell 23:265–279.

Geng LN, Yao Z, Snider L, Fong AP, Cech JN, Young JM, van der Maarel SM, Ruzzo WL, Gentleman RC, Tawil R, Tapscott SJ. 2012. DUX4 activates germline genes, retroelements, and immune mediators: implications for facioscapulohumeral dystrophy. Dev Cell 22:38–51.

Gregson HC, Schmiesing JA, Kim J-S, Kobayashi T, Zhou S, Yokomori K. 2001. A potential role for human cohesin in mitotic spindle aster assembly. J Biol Chem 276:47575–47582.

Hansen RS, Wijmenga C, Luo P, Stanek AM, Canfield TK, Weemaes CM, Gartler SM. 1999. The DNMT3B DNA methyltransferase gene is mutated in the ICF immunodeficiency syndrome. Proc Natl Acad Sci USA 96:14412–14417.

Hewitt JE, Lyle R, Clark LN, Valleley EM, Wright TJ, Wijmenga C, van Deutekom JC, Francis F, Sharpe PT, Hofker M, Frants RR, Williamson R. 1994. Analysis of the tandem repeat locus D4Z4 associated with facioscapulohumeral muscular dystrophy. Hum Mol Genet 3:1287–1295.

Iwasa E, Hamashima Y, Fujishiro S, Higuchi E, Ito A, Yoshida M, Sodeoka M. 2010. Total synthesis of (+)-chaetocin and its analogues: their histone methyltransferase G9a inhibitory activity. J Am Chem Soc 132:4078–4079.

Jones TI, Chen JC, Rahimov F, Homma S, Arashiro P, Beermann ML, King OD, Miller JB, Kunkel LM, Emerson CPJ, Wagner KR, Jones PL. 2012. Facioscapulohumeral muscular dystrophy family studies of DUX4 expression: evidence for disease modifiers and a quantitative model of pathogenesis. Hum Mol Genet 21:4419–4430.

Krom YD, Thijssen PE, Young JM, den Hamer B, Balog J, Yao Z, Maves L, Snider L, Knopp P, Zammit PS, Rijkers T, van Engelen BG, et al. 2013. Intrinsic epigenetic regulation of the D4Z4 macrosatellite repeat in a transgenic mouse model for FSHD. PLoS Genet 9:e1003415.

Lemmers RJ, de Kievit P, Sandkuijl L, Padberg GW, van Ommen GJ, Frants RR, van der Maarel SM. 2002. Facioscapulohumeral muscular dystrophy is uniquely associated with one of the two variants of the 4q subtelomere. Nat Genet 32:235–236.

Lemmers RJ, van der Vliet PJ, Klooster R, Sacconi S, Camaño P, Dauwerse JG, Snider L, Straasheijm KR, van Ommen GJ, Padberg GW, Miller DG, Tapscott SJ, et al. 2010a. A unifying genetic model for facioscapulohumeral muscular dystrophy. Science 329:1650–1653.

Lemmers RJ, van der Vliet PJ, van der Gaag KJ, Zuniga S, Frants RR, de Knijff P, van der Maarel SM. 2010b. Worldwide population analysis of the 4q and 10q subtelomeres identifies only four discrete interchromosomal sequence transfers in human evolution. Am J Hum Genet 86:364–377.

Lemmers RJ, Wohlgemuth M, Frants RR, Padberg GW, Morava E, van der Maarel SM. 2004. Contractions of D4Z4 on 4qB subtelomeres do not cause facioscapulohumeral muscular dystrophy. Am J Hum Genet 75:1124–1130.

Lemmers RJ, Wohlgemuth M, van der Gaag KJ, van der Vliet PJ, van Teijlingen CM, de Knijff P, Padberg GW, Frants RR, van der Maarel SM. 2007. Specific sequence variations within the 4q35 region are associated with facioscapulohumeral muscular dystrophy. Am J Hum Genet 81:884–894.

Lemmers RJL, de Kievit P, van Geel M, van der Wielen MJ, Bakker E, Padberg GW, Frants RR, van der Maarel SM. 2001. Complete allele information in the diagnosis of facioscapulohumeral muscular dystrophy by triple DNA analysis. Ann Neurol 50:816–819.

Lemmers RJLF, Tawil R, Petek LM, Balog J, Block GJ, Santen GWE, Amell AM, van der Vliet PJ, Almomani R, Straasheijm KR, Krom YD, Klooster R, et al. 2012. Digenic inheritance of an SMCHD1 mutation and an FSHD-permissive D4Z4 allele causes facioscapulohumeral muscular dystrophy type 2. Nat Genet 44:1370–1374.

Liao D. 1999. Concerted evolution: molecular mechanism and biological implications. Am J Hum Genet 64:24–30.

Lyle R, Wright TJ, Clark LN, Hewitt JE. 1995. The FSHD-associated repeat, D4Z4, is a member of a dispersed family of homeobox-containing repeats, subsets of which are clustered on the short arms of the acrocentric chromosomes. Genomics 28:389–397.

Mitsuhashi H, Mitsuhashi S, Lynn-Jones T, Kawahara G, Kunkel LM. 2013. Expression of DUX4 in zebrafish development recapitulates facioscapulohumeral muscular dystrophy. Hum Mol Genet 22:568–577.

Mostert V, Hill KE, Burk RF. 2003. Loss of activity of the selenoenzyme thioredoxin reductase causes induction of hepatic heme oxygenase-1. FEBS Lett 541:85–88.

Mugal CF, Ellegren H. 2011. Substitution rate variation at human CpG sites correlates with non-CpG divergence, methylation level and GC content. Genome Biol 12:R58.

Nozawa RS, Nagao K, Igami KT, Shibata S, Shirai N, Nozaki N, Sado T, Kimura H, Obuse C. 2013. Human inactive X chromosome is compacted through a PRC2-independent SMCHD1-HBiX1 pathway. Nat Struc Mol Biol 20:566–573.

Rahimov F, King OD, Leung DG, Bibat GM, Emerson CPJ, Kunkel LM, Wagner KR. 2012. Transcriptional profiling in facioscapulohumeral muscular dystrophy to identify candidate biomarkers. Proc Natl Acad Sci USA 109:16234–16239.

Rideout WMr, Coetzee GA, Olumi AF, Jones PA. 1990. 5-Methylcytosine as an endogenous mutagen in the human LDL receptor and p53 genes. Science 249:1288–1290.

Sacconi S, Lemmers RJ, Balog J, van der Vliet PJ, Lahaut P, van Nieuwenhuizen MP, Straasheijm KR, Debipersad RD, Vos-Versteeg M, Salviati L, Casarin A, Pegoraro E, et al. 2013. The FSHD2 gene smchd1 is a modifier of disease severity in families affected by FSHD1. Am J Hum Genet 93:744–751.

Scionti I, Greco F, Ricci G, Govi M, Arashiro P, Vercelli L, Berardinell iA, Angelini C, Antonini G, Cao M, Di Muzio A, Moggio M, et al. 2012. Large-scale population analysis challenges the current criteria for the molecular diagnosis of fascioscapulohumeral muscular dystrophy. Am J Hum Genet 90:628–635.

Sharon N, Mor I, Zahavi E, Benvenisty N. 2012. DUXO, a novel double homeobox transcription factor, is a regulator of the gastrula organizer in human embryonic stem cells. Stem Cell Res 9:261–269.

Shiomi K, Kiyono T, Okamura K, Uezumi M, Goto Y, Yasumoto S, Shimizu S, Hashimoto N. 2011. CDK4 and cyclin D1 allow human myogenic cells to recapture growth property without compromising differentiation potential. Gene Ther 18:857–866.

Snider L, Asawachaicharn A, Tyler AE, Geng LN, Petek LM, Maves L, Miller DG, Lemmers RJ, Winokur ST, Tawil R, van der Maarel SM, Filippova GN, et al. 2009. RNA transcripts, miRNA-sized fragments and proteins produced from D4Z4 units: new candidates for the pathophysiology of facioscapulohumeral dystrophy. Hum Mol Genet 18:2414–2430.

Snider L, Geng LN, Lemmers RJ, Kyba M, Ware CB, Nelson AM, Tawil R, Filippova GN, van der Maarel SM, Tapscott SJ, Miller DG. 2010. Facioscapulohumeral dystrophy: incomplete suppression of a retrotransposed gene. PLoS Genet 6:e1001181.

Tam R, Smith KP, Lawrence JB. 2004. The 4q subtelomere harboring the FSHD locus is specifically anchored with peripheral heterochromatin unlike most human telomeres. J Cell Biol 167:269–279.

Thijssen PE, Tobi EW, Balog J, Schouten SG, Kremer D, Bouazzaoui FE, Henneman P, Putter H, Slagboom PE, Heijmans BT, van der Maarel SM. 2013. Chromatin remodeling of human subtelomeres and TERRA promoters upon cellular senescence: commonalities and differences between chromosomes. Epigenetics 8:512–521.

Tibodeau JD, Benson LM, Isham CR, Owen WG, Bible KC. 2009. The anticancer agent chaetocin is a competitive substrate and inhibitor of thioredoxin reductase. Antioxid Redox Signal 11:1097–1106.

Trigona WL, Mullarky IK, Cao Y, Sordillo LM. 2006. Thioredoxin reductase regulates the induction of haem oxygenase-1 expression in aortic endothelial cells. Biochem J 394:207–216.

Turki A, Hayot M, Carnac G, Pillard F, Passerieux E, Bommart S, Raynaud de Mauverger E, Hugon G, Pincemail J, Pietri S, Lambert K, Belayew A, et al. 2012. Functional muscle impairment in facioscapulohumeral muscular dystrophy is correlated with oxidative stress and mitochondrial dysfunction. Free Radic Biol Med 53:1068–1079.

van der Maarel SM, Frants RR. 2005. The D4Z4 repeat-mediated pathogenesis of facioscapulohumeral muscular dystrophy. Am J Hum Genet 76:375–386.

van der Maarel SM, Tawil R, Tapscott SJ. 2011. Facioscapulohumeral muscular dystrophy and DUX4: breaking the silence. Trends Mol Med 17:252–258.

Vanderplanck C, Ansseau E, Charron S, Stricwant N, Tassin A, Laoudj-Chenivesse D, Wilton SD, Coppée F, Belayew A. 2011. The FSHD atrophic myotube phenotype is caused by DUX4 expression. PLoS One 6:e26820.

van Overveld PG, Lemmers RJ, Sandkuijl LA, Enthoven L, Winokur ST, Bakels F, Padberg GW, van Ommen G-JB, Frants RR, van der Maarel SM. 2003. Hypomethylation of D4Z4 in 4q-linked and non-4q-linked facioscapulohumeral muscular dystrophy. Nat Genet 35:315–317.

Weber M, Davies JJ, Wittig D, Oakeley EJ, Haase M, Lam WL, Schübeler D. 2005. Chromosome-wide and promoter-specific analyses identify sites of differential DNA methylation in normal and transformed human cells. Nat Genet 37:853–862.

Winokur ST, Bengtsson U, Feddersen J, Mathews KD, Weif-fenbach B, Bailey H, *Markovich RP, Murray JC, Wasmuth JJ, Altherr MR.* 1994. *The DNA rear*rangement associated with facioscapulohumeral muscular dystrophy involves a heterochromatin-associated repetitive element: implications for a role of chromatin structure in the pathogenesis of the disease. Chromosome Res 2:225–234.

Winokur ST, Bengtsson U, Vargas JC, Wasmuth JJ, Altherr MR, Weiffenbach B, Jacobsen SJ. 1996. The evolutionary distribution and structural organization of the homeoboxs-containing repeat D4Z4 indicates a functional role for the ancestral copy in the FSHD region. Hum Mol Genet 5:1567–1575.

Xia J, Han L, Zhao Z. 2012. Investigating the relationship of DNA methylation with mutation rate and allele frequency in the human genome. BMC Genomics 13:S7.

Xu GL, Bestor TH, Bourc'his D, Hsieh CL, Tommerup N, Bugge M, Hulten M, Qu X, Russo JJ, Viegas-Pequignot E. 1999. Chromosome instability and immunodeficiency syndrome caused by mutations in a DNA methyltransferase gene. Nature 402:187–191.

Zeng W, de Greef JC, Chen Y-Y, Chien R, Kong X, Gregson HC, Winokur ST, Pyle A, Robertson KD, Schmiesing JA, Kimonis VE, Balog J, et al. 2009. Specific loss of histone H3 lysine 9 trimethylation and HP1γ/cohesin binding at D4Z4 repeats is associated with facioscapulohumeral dystrophy (FSHD). PLoS Genet 5:e1000559.

Zhang Y, Forner J, Fournet S, Jeanpierre M. 2001. Improved characterization of FSHD mutations. Ann Genet 44:105–110.

Geriat. Med. 52(8) : 893～895, 2014

特集　高齢者の薬物療法ガイドライン

総説

1．薬物療法ガイドラインにおける高齢者の扱いについて

江頭　正人

KEY WORD　■高齢者　■薬物療法　■動脈硬化性疾患予防ガイドライン 2012 年版　■高血圧治療ガイドライン 2014

SUMMARY

■高齢患者の爆発的増加に従って，診療ガイドラインにおいても高齢者をどのように診療すべきか，に関する記載が増えてきている．高齢者が一般成人とは異なる対応が必要となることはいうまでもないが，具体的にどのようにすべきか，日常診療におけるクリニカルクエッションにこたえられるだけのエビデンスは質・量ともに不十分であり，今後の研究の進展が必須である．

はじめに

多くの臨床試験において，高齢者，特に 75～80 歳以上の高齢者は，併発症や臓器障害の合併などの理由で対象から除外されているか，あるいは除外されていなくてもエントリー基準を満たさない場合が多く，わずかな数しか参加していない．したがって，後期高齢者において疾患治療にどのような方法がよいのか，臨床試験にて効果が確認されている方法は限られており，そのことが多くのガイドラインにも特記事項として記載されている．一方，高齢者においては，生命予後や重大なイベントを防ぐことはもちろん重要であるが，それ以外に，日常生活機能や認知機能を維持し要介護にならないことも重要なエンドポイントと考えられるが，そのことを検証した臨床試験はやはり数少ない．さらに，既に生活機能が低下している高齢者が，元気な自立した高齢者と同じ対応でよいのかどうかも不明なことが多く，十分な研究はされていないと考えられる．また，一般成人と比べて薬物有害事象が起きやすいことから，薬物療法のリスク・ベネフィットのバランスも一般成人とは異なる可能性がある．本稿において，わが国の代表的な診療ガイドラインである『動脈硬化性疾患予防ガイドライン 2012 年版』と『高血圧治療ガイドライン 2014』を例にとり，高齢者に関してどのような記載がなされているのか概説する．

『動脈硬化性疾患予防ガイドライン 2012 年版』　日本動脈硬化学会

『動脈硬化性疾患予防ガイドライン 2012 年版』において，高齢者に関する記載が 1 章設けられており，ステートメントとして以下のような記載がなされている．その中で，前期高齢者(65 歳以上 75 歳未満)では，高 LDL コレステロール血症が冠動脈疾患の危険因子であること，スタチンによる LDL コレステロール低下療法により冠動脈疾患の 1 次予防，2 次予防，脳梗塞の 1 次予防が期待し得ることが推奨されている(推奨レベルⅡa：どちらかというと有用，効用あり)．後期高齢者(75 歳以上)についていえば，高 LDL コレステロール血症に対するスタチンによる LDL コレステロール低下療法で，

■えとう　まさと(東京大学医学部附属病院総合研修センター)

冠動脈疾患の2次予防効果が期待できるが(推奨レベルⅡa)，1次予防効果は明らかではなく，主治医の判断で個々の患者に対応する，と記載されている．

実際に，高齢者における高LDLコレステロール血症の動脈硬化性疾患の危険因子としての位置づけについては，後期高齢者でも有意なリスクになり得るが，その程度は一般成人におけるほど強くない[1]．介入試験についていえば，70歳以上高齢者を対象とした臨床試験はPROSPERのみであり，スタチンにより冠動脈疾患の死亡＋非致死性心筋梗塞のリスクは，有意に19%低下することが報告されている[2]．しかしながら，本試験のサブ解析において，2次予防患者では効果が認められたが，1次予防患者では効果が認められていなかった．このようなエビデンスを基に，高齢者のステートメントが作成されている．

加えて，高齢者治療の留意点についても記載されている．その中で高齢者の特徴として，動脈硬化性疾患以外の生命予後に影響する複数疾患の合併，臓器障害の潜在，臓器予備能の低下，症候の非定型性，薬物代謝能の低下などを挙げている．薬物治療については，上記のような高齢者の特徴を基盤として薬物有害事象が出現しやすくなっていることから，安易な適応に注意を喚起している．後期高齢者の高LDLコレステロール血症に関しては，上記のように十分なエビデンスがないことから，個々の患者の病態を十分に検討し，主治医の判断で柔軟に対応すべきであること，また今後の研究を進めるべきであることが強調されている．

高齢者における重要なエンドポイントである認知症のリスクを，高LDLコレステロール血症の治療により低下させ得るかどうかについて，本ガイドラインでは記載はない．日本神経学会が中心となり作成された『認知症疾患治療ガイドライン2010』においては，「高コレステロール血症治療薬は認知症予防に有用か？」というクリニカルクエッションに対し，中年期の高コレステロール血症はアルツハイマー病の危険因子であるが，高齢者では高コレステロール血症とアルツハイマー病の関連は明確でなく，スタチンを用いた介入試験において，認知機能の低下や認知症の発症予防が認められなかったことから，スタチンの認知症予防目的の投与は慎重を要すると記載されている．

『高血圧治療ガイドライン2014』日本高血圧学会

『高血圧治療ガイドライン2014』において，高齢者に関する記載が1章設けられており，ステートメントとして以下のような記載がなされている．原則として140/90 mmHg以上の血圧レベルを薬物治療の対象として推奨する．ただし，75歳以上で収縮期血圧140～149 mmHgや6m歩行が完遂できない程度のフレイルな高齢者では，個別に判断する(推奨グレードB：科学的根拠があり行うよう勧められる)．また降圧目標に関しては，65～74歳に関しては140/90 mmHg未満，75歳以上であれば150/90 mmHg未満とし，忍容性あれば積極的に140/90 mmHg未満を目指す，と記載されている(推奨グレードB)．さらに高齢者の薬物療法に当たっての注意点として，副作用の発現や臓器障害に留意し，QOLに配慮しながら時間をかけて緩徐に降圧する，と記載されている．

実際に高齢者であっても，基本的には血圧が低いほど心血管リスクは低いことが疫学研究から示されており[3]，このことから血圧基準は非高齢者と同じとされている．薬物療法の効果に関しては，60歳以上の高血圧患者を対象とした臨床試験のメタ解析において，降圧薬による治療はプラセボに対して全死亡リスクを12%，脳卒中発症リスクを35%，冠動脈疾患発症リスクを15%有意に減少させることが報告されている[4]．また，80歳以上の比較的元気な高齢高血圧患者を対象としたHYVETにおいては，降圧利尿薬をメインとした降圧薬投与にて150/80 mmHg未満を目指した治療の結果，プラセボと比較して脳卒中リスクが30%，全死亡リスクが21%，心不全発症リスクが64%の有意な減少が報告されている[5]．

治療対象に関しては，降圧治療の有用性が示

されたランダム化比較試験では，収縮期血圧160 mmHg以上が登録基準とされているものが多く，少なくとも75歳以上の高齢者において，収縮期血圧で140～149 mmHg以上を治療対象とすることの有用性を示したエビデンスは存在しない．イギリスのNICEのガイドラインでは，80歳以上の高齢高血圧患者の降圧薬治療の対象を160/100 mmHg以上としている．ヨーロッパのESH/ESCのガイドライン2013では，高齢者では収縮期血圧が160 mmHg以上であれば降圧薬が推奨され，80歳未満であれば140～159 mmHgで降圧薬治療を考慮してもよいとされ，80歳以上で140～159 mmHgの場合は個別に判断すべきとされている．さらに降圧治療の適応を，フレイルの程度に応じて個別に設定すべきであることを示唆する観察研究も報告されている[6]．6 m歩行において0.8 m/秒以上の速度で歩ける元気な高齢者は，高血圧の存在が生命予後の悪化と関連するが，6 m歩行を完遂できないフレイルな高齢者は，むしろ血圧が高い方が生命予後はよかったと報告されている．歩行速度は，高齢者におけるフレイルな状態を示す重要なマーカーであり，フレイルな高齢者では高血圧の管理の仕方を変える必要があることを示唆している．

高齢者における重要なエンドポイントである認知症に関しては，高齢者とは別に1章設けられている．その中でステートメントとして，中年期の高血圧は高齢期認知症の危険因子であり，積極的に治療すべきてあるとされている(推奨グレードC1：科学的根拠は不十分だが行うよう勧められる)．一方で，高齢期の高血圧に対する降圧療法が認知症リスクを下げるかどうかは明らかではないが，認知機能を悪化させるとする報告はないと記載されている．また，認知症合併高血圧患者に対する降圧療法の有用性に関するエビデンスはほとんどなく，降圧治療に当たっては薬物アドヒアランスに注意を払い，処方の単純化や介護スタッフによる服薬管理などの工夫を行うとされている．また，『認知症疾患治療ガイドライン2010』においてもほぼ同様に，中年期の高血圧は高齢期の認知症ないしアルツハイマー病の危険因子であり積極的に治療すべきであるが，高齢期の認知症と高血圧の関連は明確でなく，高齢期における認知症予防のための降圧目標は定まっていないとされている．

文　献

1) Prospective Studies Collaboration：Blood cholesterol and vascular mortality by age, sex, and blood pressure：a meta-analysis of individual data from 61 prospective studies with 55,000 vascular deaths. Lancet 2007；**370**：1829-1839.
2) Shepherd J et al：PROSPER study group. PROspective Study of Pravastatin in the Elderly at Risk：Pravastatin in elderly individuals at risk of vascular disease (PROSPER)：a randomised controlled trial. Lancet 2002；**360**：1623-1630.
3) Lewington S et al：Prospective Studies Collaboration：Age-specific relevance of usual blood pressure to vascular mortality：a meta-analysis of individual data for one million adults in 61 prospective studies. Lancet 2002；**360**：1903-1913.
4) Insua JT et al：Drug treatment of hypertension in the elderly：a meta-analysis. Ann Intern Med 1994；**121**：355-362.
5) Beckett NS et al；HYVET Study Group：Treatment of hypertension in patients 80 years of age or older. N Engl J Med 2008；**358**：1887-1898.
6) Odden MC et al：Rethinking the association of high blood pressure with mortality in elderly adults：the impact of frailty. Arch Intern Med 2012；**172**：1162-1168.

(執筆者連絡先)　江頭正人　〒113-8655　東京都文京区本郷7-3-1　東京大学医学部附属病院総合研修センター